

MARTIN MARIETTA ENERGY SYSTEMS LIBRARIES



3 4456 0286019 8

NUREG/CR-3171
(ORNL/TM-8667)

ornl

**OAK
RIDGE
NATIONAL
LABORATORY**

**UNION
CARBIDE**

Data Summary Report for Fission Product Release Test Hi-2

**M. F. Osborne
R. A. Lorenz
J. R. Travis
C. S. Webster
K. S. Norwood**

OAK RIDGE NATIONAL LABORATORY

CENTRAL RESEARCH LIBRARY

CIRCULATION SECTION

4500N ROOM 175

LIBRARY LOAN COPY

DO NOT TRANSFER TO ANOTHER PERSON

If you wish someone else to see this
report, send in name with report and
the library will arrange a loan.

UCN-7969 3 9-771

**Prepared for the
U.S. Nuclear Regulatory Commission
Office of Nuclear Regulatory Research
Under Interagency Agreement DOE 40-551-75**

**OPERATED BY
UNION CARBIDE CORPORATION
FOR THE UNITED STATES
DEPARTMENT OF ENERGY**

Printed in the United States of America. Available from
National Technical Information Service
U.S. Department of Commerce
5285 Port Royal Road, Springfield, Virginia 22161

Available from
GPO Sales Program
Division of Technical Information and Document Control
U.S. Nuclear Regulatory Commission
Washington, D.C. 20555

This report was prepared as an account of work sponsored by an agency of the United States Government. Neither the United States Government nor any agency thereof, nor any of their employees, makes any warranty, express or implied, or assumes any legal liability or responsibility for the accuracy, completeness, or usefulness of any information, apparatus, product, or process disclosed, or represents that its use would not infringe privately owned rights. Reference herein to any specific commercial product, process, or service by trade name, trademark, manufacturer, or otherwise, does not necessarily constitute or imply its endorsement, recommendation, or favoring by the United States Government or any agency thereof. The views and opinions of authors expressed herein do not necessarily state or reflect those of the United States Government or any agency thereof.

NUREG/CR-3171
ORNL/TM-8667
Dist. Category R3

Chemical Technology Division

DATA SUMMARY REPORT FOR FISSION PRODUCT RELEASE TEST HI-2

M. F. Osborne
R. A. Lorenz
J. R. Travis
C. S. Webster
K. S. Norwood*

*Guest scientist from UKAEA.

Manuscript Completed — January 1983
Date of Issue — February 1984

NOTICE This document contains information of a preliminary nature.
It is subject to revision or correction and therefore does not represent a
final report.

Prepared for the
U.S. Nuclear Regulatory Commission
Office of Nuclear Regulatory Research
Under Interagency Agreement DOE 40-551-75

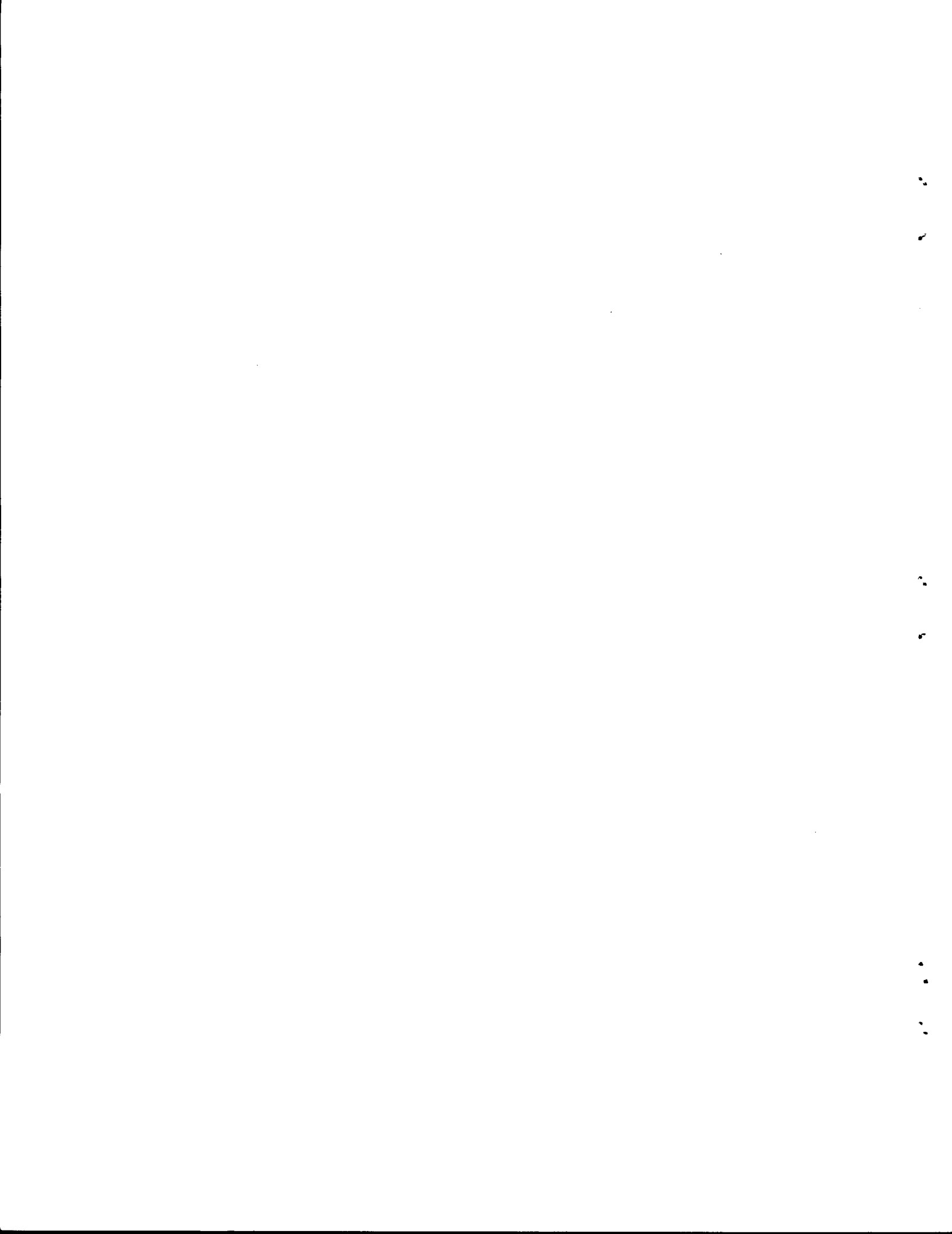
NRC FIN No. B0127

Prepared by the
OAK RIDGE NATIONAL LABORATORY
Oak Ridge, Tennessee 37831
operated by
UNION CARBIDE CORPORATION
for the
U.S. DEPARTMENT OF ENERGY
Under Contract No. W-7402-eng-26

MARTIN MARIETTA ENERGY SYSTEMS LIBRARIES



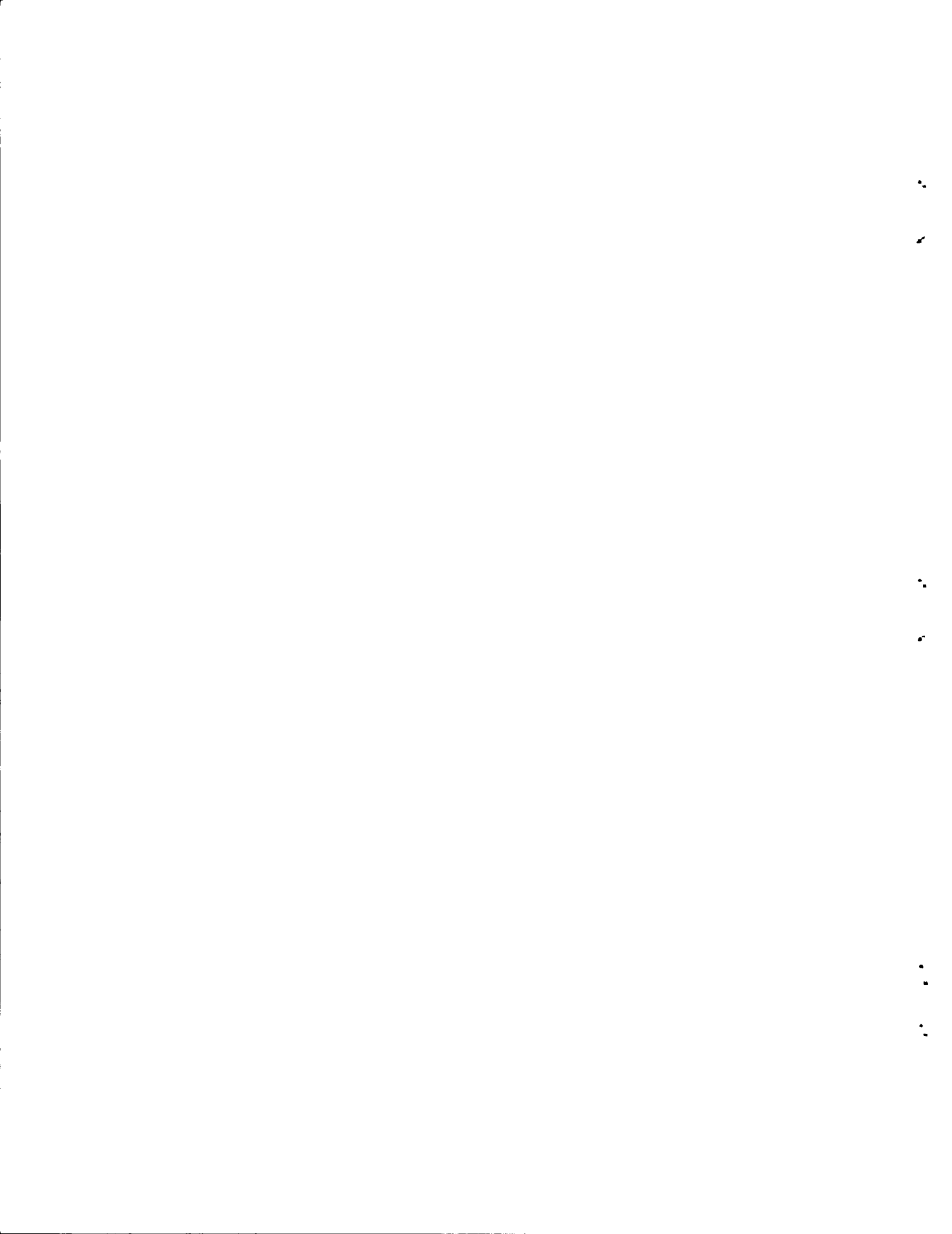
3 4456 0286019 8



ABSTRACT

The second in a series of high-temperature fission product release tests was conducted for 20 min at about 1700°C in flowing steam. The test specimen, a 20-cm-long section of an H. B. Robinson fuel rod that had been irradiated to a burnup of 28,000 MWd/t, was heated in an induction furnace mounted in a hot cell.

Posttest analyses of the furnace, the thermal gradient tube, filters, and other components of the experimental apparatus showed that about 50% of the ^{85}Kr , ^{137}Cs , and ^{129}I were released from the specimen during the test. In addition, approximately 2% of the $^{110\text{m}}\text{Ag}$ and ^{125}Sb along with smaller fractions of several other radionuclides were measured by gamma spectrometry. Spark-source mass spectrometric data from a limited number of samples showed significant releases of fission product tellurium and molybdenum, as well as structural (zirconium and tin) and furnace (primarily tungsten) materials. Metallographic examination of the fuel specimen revealed extensive fractures in the cladding, essentially complete oxidation to ZrO_2 , and evidence of fuel-cladding interaction.



CONTENTS

	<u>Page</u>
ABSTRACT	iii
ACKNOWLEDGMENTS	vii
LIST OF FIGURES	ix
LIST OF TABLES	xi
1. INTRODUCTION	1
2. DESCRIPTION OF TEST HI-2	2
2.1 Fuel Specimen Data	2
2.2 Experimental Apparatus	2
2.3 Test Conditions and Operation	2
2.4 Posttest Disassembly and Sample Collection	13
3. TEST RESULTS	13
3.1 Test Data	13
3.2 Posttest Data	16
3.2.1 Results from gamma spectrometry	16
3.2.2 Results of activation analysis for iodine	16
3.2.3 Results of spark-source mass spectrometric analyses	23
3.2.4 Thermal gradient tube results	26
3.2.4.1 Cesium on the thermal gradient tube	26
3.2.4.2 Iodine on the thermal gradient tube	34
3.2.4.3 Silver on the thermal gradient tube	35
3.2.4.4 Antimony on the thermal gradient tube ...	35
3.2.5 Results of analysis of cladding and end-cap samples from tests HI-1 and HI-2	36
3.2.5.1 Interpretation	36
3.2.5.2 Metallographic examination of fuel specimens	41
4. CONCLUSIONS	48
5. REFERENCES	51

•

•

•

•

•

•

•

ACKNOWLEDGMENTS

The authors gratefully acknowledge the significant contributions of several colleagues in conducting this work: J. F. Emery, D. A. Costanzo, J. Northcutt, and L. Landau of the Analytical Chemistry Division for the ^{129}I determinations and spark-source mass spectrometry; L. Shrader of the Metals and Ceramics Division for metallographic examination; R. P. Wichner and T. B. Lindemer for technical consultation; B. C. Drake for preparation of the manuscript; and M. G. Stewart for editing.



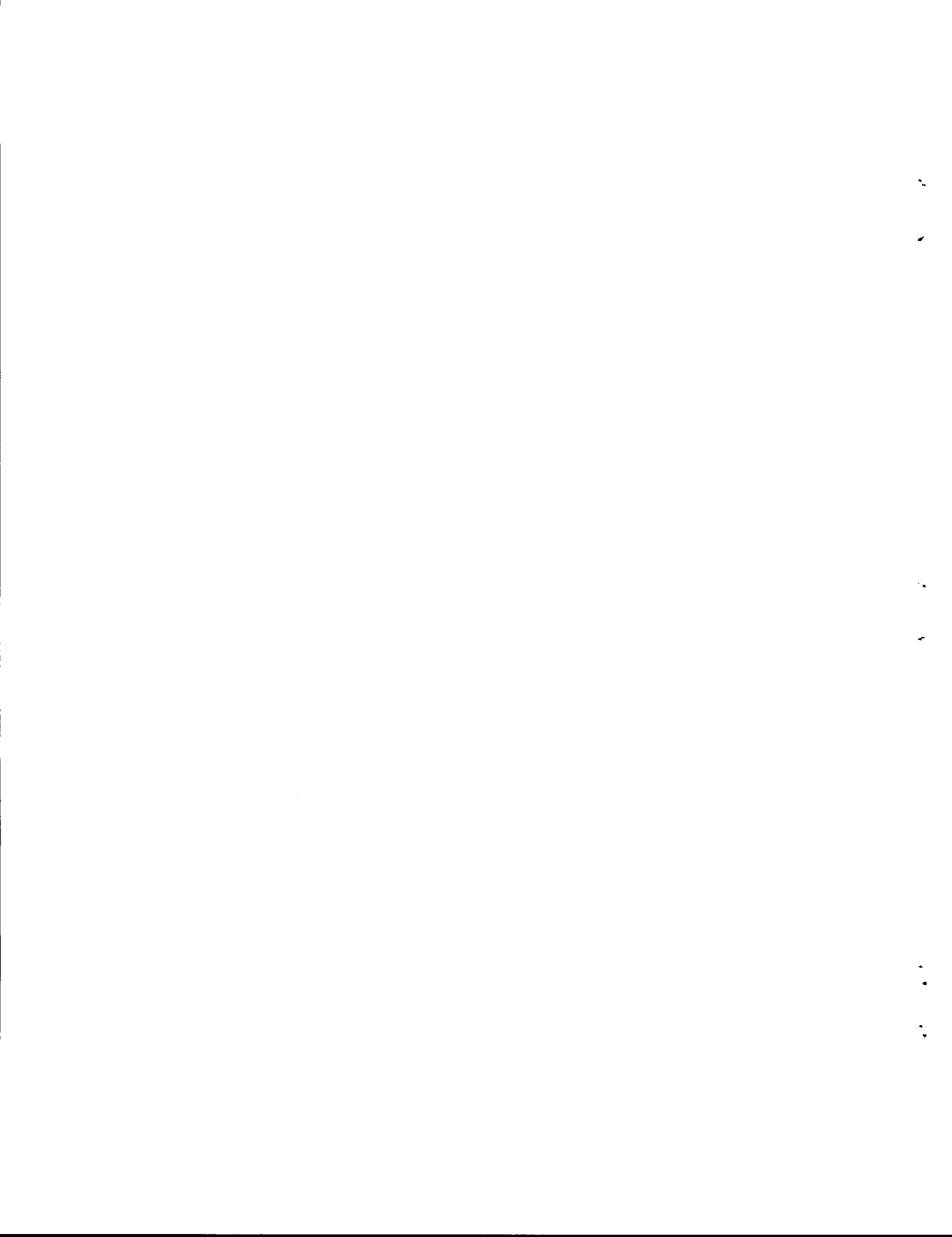
LIST OF FIGURES

<u>Number</u>	<u>Page</u>
1. Gamma profile of fuel rod H-15, showing locations of cuts; section A-8 was used in test HI-2	6
2. Fuel specimen for fission product release studies	7
3. Fission product release furnace	8
4. Fission product release and collection system	9
5. Photograph of (a) fission product release furnace, (b) thermal gradient tube, and (c) filter package in steel containment box before test HI-2	10
6. Data acquisition and processing system for fission product release test	11
7. Two unirradiated fuel specimens, illustrating the appearance before and after heating at 1700°C in steam	14
8. Temperature and flow history of test HI-2	15
9. Release of cesium and krypton as functions of time and temperature in test HI-2	17
10. Distribution of fission products in test HI-2	22
11. Temperature distribution along thermal gradient tube, test HI-2	27
12. Mass of cesium in thermal gradient tube after test HI-2	28
13. Mass of iodine in thermal gradient tube after test HI-2	31
14. Mass of silver on thermal gradient tube after test HI-2	32
15. Mass of antimony in thermal gradient tube after test HI-2 ...	33
16. Appearance of metallographic specimen from test HI-1, showing cladding fractures and ZrO ₂ boat (~4.8x)	42
17. Comparison of (a) cladding appearance in irradiated but untested control specimen with (b) that in test HI-1. Note fracture, the increase in thickness, and the ZrO ₂ and α-ZrO layers resulting from the conditions used for the test	43
18. Appearance of test HI-1 specimen under polarized light, which makes grain structures visible	44

<u>Number</u>	<u>Page</u>
19. Appearance of metallographic specimen from test HI-2, showing wide opening at cladding fracture (~5x)	45
20. Sketch of HI-2 fuel specimen after test, showing large longitudinal fracture, unidentified dark spot on downstream end of specimen, and locations of cuts for metallographic examination	46
21. Completely oxidized cladding adjacent to fracture in test HI-2	47
22. Higher-magnification view from central region of test HI-2 cladding, showing precipitates of metallic tin	49
23. Area of apparent fuel-cladding interaction in test HI-2, showing chip of UO ₂ fuel adhering to oxidized Zircaloy cladding	50

LIST OF TABLES

<u>Number</u>	<u>Page</u>
1. Data for fuel specimen used in test HI-2	3
2. Amounts of principal fission and activation product elements in H. B. Robinson fuel after 2627 d of decay	4
3. Principal radionuclides and selected stable nuclides in H. B. Robinson fuel after 2627 d of decay	5
4. Operating conditions for test HI-2	12
5. Distribution of fission products released in test HI-2	18
6. Distribution of cesium in test HI-2	19
7. Distribution of antimony in test HI-2	20
8. Distribution of silver in test HI-2	21
9. Distribution of iodine in test HI-2 (Results of activation analysis for ¹²⁹ I)	24
10. Results of spark-source mass spectrometry of samples from test HI-2 components	25
11. Fission products on thermal gradient tube sections before and after leaching	29
12. Fission products on HI-2 thermal gradient tube	30
13. Activities of cladding and end-cap samples from test HI-1	37
14. Activities of cladding and end-cap samples from test HI-2	38
15. Enrichment of nuclide relative to fuel dust (¹⁴⁴ Ce and ¹⁵⁴ Eu) in HI-1	40
16. Enrichment of nuclide relative to fuel dust (¹⁴⁴ Ce) in HI-2	40



DATA SUMMARY REPORT FOR FISSION PRODUCT RELEASE TEST HI-2

M. F. Osborne
R. A. Lorenz
J. R. Travis
C. S. Webster
K. S. Norwood

1. INTRODUCTION

This was the second test in a series designed to investigate fission product release from LWR fuel in steam throughout the temperature range 1400 to ~2400°C.¹ Earlier tests, which were conducted under similar conditions at temperatures of 500 to 1600°C, have been reported by Lorenz et al.²⁻⁵ The purpose of this work, which is sponsored by the U.S. Nuclear Regulatory Commission (NRC), is to obtain the experimental data needed to reliably assess the consequences of heatup accidents in light water reactors (LWRs). The overall objectives of this program are:

1. to determine the extent of fission product release from discharged LWR fuel at temperatures up to and including fuel melting (~2400°C);
2. to identify the chemical species released in both the gas and the condensed phases, if possible;
3. to collect and characterize the aerosols released;
4. to correlate the results with data from related programs and develop a consistent source-term model applicable to any LWR fuel subjected to a spectrum of accident conditions; and
5. to aid in the interpretation of integral melt tests at ORNL (LWR Aerosol Release and Transport Program) and of tests with simulated fuel only (SASCHA Program at Karlsruhe, Germany).

Tests of fully irradiated LWR fuel will be emphasized in this program, but the applicability of simulated fuel (unirradiated UO₂ containing a range of fission product elements) will be investigated in the higher-temperature tests (>2000°C). All tests will be performed in a flowing mixture of steam and argon (or helium) at atmospheric pressure; steam concentrations will be varied to simulate different accident sequences.

Test temperatures in the existing induction furnace will be limited to a maximum of about 2000°C. Higher-temperature tests will require the replacement of the currently used ZrO₂ ceramics with ThO₂. The existing fission product collection and analysis system will be improved to provide chemical species identification when suitable instrumentation (laser-induced fluorescence spectrometry is under development) is available.

This second data summary report is intended to provide a brief description of test HI-2 and to tabulate the data obtained. As noted in

the first data summary report,⁶ a thorough data evaluation and correlation will be included in a subsequent topical report covering several fission product release tests.

2. DESCRIPTION OF TEST HI-2

The objective of test HI-2 was to obtain fission product release data under strongly oxidizing conditions at 1700°C for a period of 20 min.

2.1 Fuel Specimen Data

The fuel specimen used in the test was a 20.3-cm (8-in.)-long section from rod H-15 of bundle B05, which operated in the Carolina Power and Light Company's H. B. Robinson 2 Reactor from October 1971 to May 1974.⁷ Details of the irradiation and the characteristics of this particular specimen are listed in Table 1; fission product inventories for this specimen are shown in Tables 2 and 3.

The specimen was cut from section A-8 of rod H-15; Fig. 1 shows the location with respect to the gamma-ray profile (which is an indication of the burnup profile). Tapered Zircaloy-2 end caps were pressed onto the ends of the specimen, not to serve as gas seals but to prevent loss of the fractured UO₂ fuel during subsequent handling. A small hole, 1.6 mm (0.063 in.) in diameter, was drilled through the cladding at midlength to serve as a standard leak for fission product escape during the heatup phase of the test. These details are illustrated in Fig. 2.

2.2 Experimental Apparatus

The fuel specimen was heated in an induction furnace, as illustrated in Fig. 3. This furnace was developed from designs used in previous experimental efforts: fission product release tests,²⁻⁴ fuel rod burst experiments,⁸ and molten fuel tests.⁹ The furnace is mounted inside a stainless steel containment box in a hot cell, as shown in Figs. 4 and 5. In test HI-2, the fission product collection system included a platinum-gold thermal gradient tube, fiberglass filters, heated charcoal (for iodine adsorption), and cooled charcoal (for rare-gas adsorption). The steam was collected in a condenser and a dryer, as indicated, prior to reaching the cooled charcoal. Instrumentation included thermocouples and an optical pyrometer for temperature measurement, NaI(Tl) radiation detectors connected to multichannel analyzers, and conventional electrical and gas flow instruments. A data acquisition system (Fig. 6) was used to record test data at 1-min intervals, and several individual chart recorders maintained continuous records of temperatures and flow rates.

2.3 Test Conditions and Operation

The operating conditions of the test are listed in Table 4. Since the hot cell and test apparatus were uncontaminated, the experimental apparatus was prepared by direct handling. Master-slave manipulators were used for transferring and loading the highly radioactive fuel specimen, as

Table 1. Data for fuel specimen used in test HI-2

Fuel rod identification	Rod H-15, bundle B05, H. B. Robinson 2 (PWR)
Irradiation data	
Period	October 1971 to May 1974
Maximum linear heat rating, peak (December 1971)	32.6 kW/m (9.95 kW/ft)
Rod average	23.3 kW/m (7.10 kW/ft)
End linear heat rating, peak (May 1974)	21.2 kW/m (6.45 kW/ft)
Rod average	17.5 kW/m (5.34 kW/ft)
Rod fuel loading	2495.4 g UO ₂ (2199.6 g U)
Burnup, rod peak	31,000 MWd/t
Burnup, test specimen	28,000 MWd/t
Specimen data	
Length	20.3 cm (8.0 in.)
Location	248 to 268 cm from bottom end of rod
Cladding OD	1.072 cm (0.422 in.)
Specimen fuel loading	135.3 g UO ₂ (119.3 g uranium)
Gas release during irradiation	0.35% of krypton; 0.25% of xenon
Total weight of specimen	166 g
Weight of Zircaloy cladding and end caps	30.7 g

Table 2. Amounts of principal fission and activation product elements in H. B. Robinson fuel after 2627 d of decay^a

Element	Amount in fuel (g/t U)	Amount in HI-2 specimen ^b (mg)
Se	47.15	5.625
Br	18.24	2.176
Kr	296.2	35.34
Rb	286.6	34.19
Sr	653.7	77.99
Y	372.2	44.40
Zr ^c	2981	355.6
Mo	2821	336.6
Tc	661.7	78.94
Ru	1885	224.9
Rh	420.8	50.20
Pd	1241	148.1
Ag	72.21	8.615
Cd	98.28	11.73
In	2.42	0.289
Sn	81.85	9.765
Sb	18.96	2.262
Te	420.8	50.20
I	208.1	24.83
Xe	4548	542.6
Cs	2087	249.0
Ba	1389	165.7
La	1027	122.5
Ce	2009	239.5
Pr	942.8	112.5
Nd	3389	404.3
Pm	19.60	2.338
Sm	703.9	83.98
Eu	117.3	13.99
Gd	93.94	11.21
Total of all fission products	28,920	3450
U	9.617×10^5	1.147×10^5
²³⁵ U	6.857×10^3	8.180×10^2
Pu	8.575×10^3	1.023×10^3

^aCalculated by C. W. Alexander on May 24, 1982, using the ORIGEN computer program and assuming a burnup of 28.0 MWd/kg and a 2627-d decay to July 15, 1981.

^bOriginal uranium content of 20.3-cm fuel specimen was 119.3 g; initial enrichment was 2.651% ²³⁵U. Thus, the fuel specimen was $119.3 \text{ g}/10^6 \text{ g} = 0.01193\%$ of a metric ton (t).

^cAmounts of zirconium and tin in the Zircaloy cladding were calculated to be $2.086 \times 10^5 \text{ g}$ and $3.13 \times 10^3 \text{ g}$ per t of initial uranium, respectively.

Table 3. Principal radionuclides and selected stable nuclides in
H. B. Robinson fuel after 2627 d of decay^a

Nuclide	Amount in fuel		Amount in HI-2 specimen ^b	
	(g/t U)	(Ci/t U)	(mg)	(mCi)
⁸³ Kr	34.66	0.0	4.135	0.0
⁸⁴ Kr	92.97	0.0	11.09	0.0
⁸⁵ Kr	12.37	4857	1.476	579.4
⁸⁶ Kr	155.4	0.0	18.54	0.0
⁹⁰ Sr ^c	367.7	50,180	43.87	5987
⁹³ Zr	597.2	1.501	71.25	0.179
⁹⁹ Tc	661.7	11.22	78.94	1.339
¹⁰⁶ Ru	1.077	3607	0.128	430.3
^{110m} Ag	5.3×10^{-4}	2.520	6.3×10^{-5}	0.301
^{113m} Cd	0.168	36.43	0.020	4.346
¹²⁵ Sb ^c	2.134	2204	0.255	262.9
¹²⁹ I	157.6	0.0278	18.80	0.0033
¹²⁸ Xe	2.470	0.0	0.295	0.0
¹³⁰ Xe	9.915	0.0	1.183	0.0
¹³¹ Xe	377.2	0.0	45.00	0.0
¹³² Xe	912.5	0.0	108.9	0.0
¹³⁴ Xe	1244	0.0	148.4	0.0
¹³⁶ Xe	2002	0.0	238.8	0.0
¹³⁴ Cs	8.372	10,840	0.999	1293
¹³⁷ Cs	860.9	74,920	102.7	8938
¹⁴⁴ Ce	0.512	1634	0.061	194.9
¹⁴⁷ Pm	19.59	18,170	2.337	2168
¹⁵¹ Sm	11.33	298.2	1.352	35.58
¹⁵⁴ Eu	18.23	4923	2.175	587.3
Total	28,920	300,900	3450	35,900

^aCalculated by C. W. Alexander on May 24, 1982, using ORIGEN computer program and assuming a burnup of 28.0 MWd/kg and a 2627-d decay to July 15, 1981.

^bOriginal uranium content of 20.3-cm fuel specimen was 119.3 g; initial enrichment was 2.651% ²³⁵U. Thus, the fuel specimen was 119.3 g/10⁶ g = 0.01193% of a metric ton.

^cFission products only; significant quantities of these and other nuclides (¹¹⁹Sn, ¹²³Sn, ⁶⁰Co, etc.) are produced by neutron activation of the Zircaloy cladding.

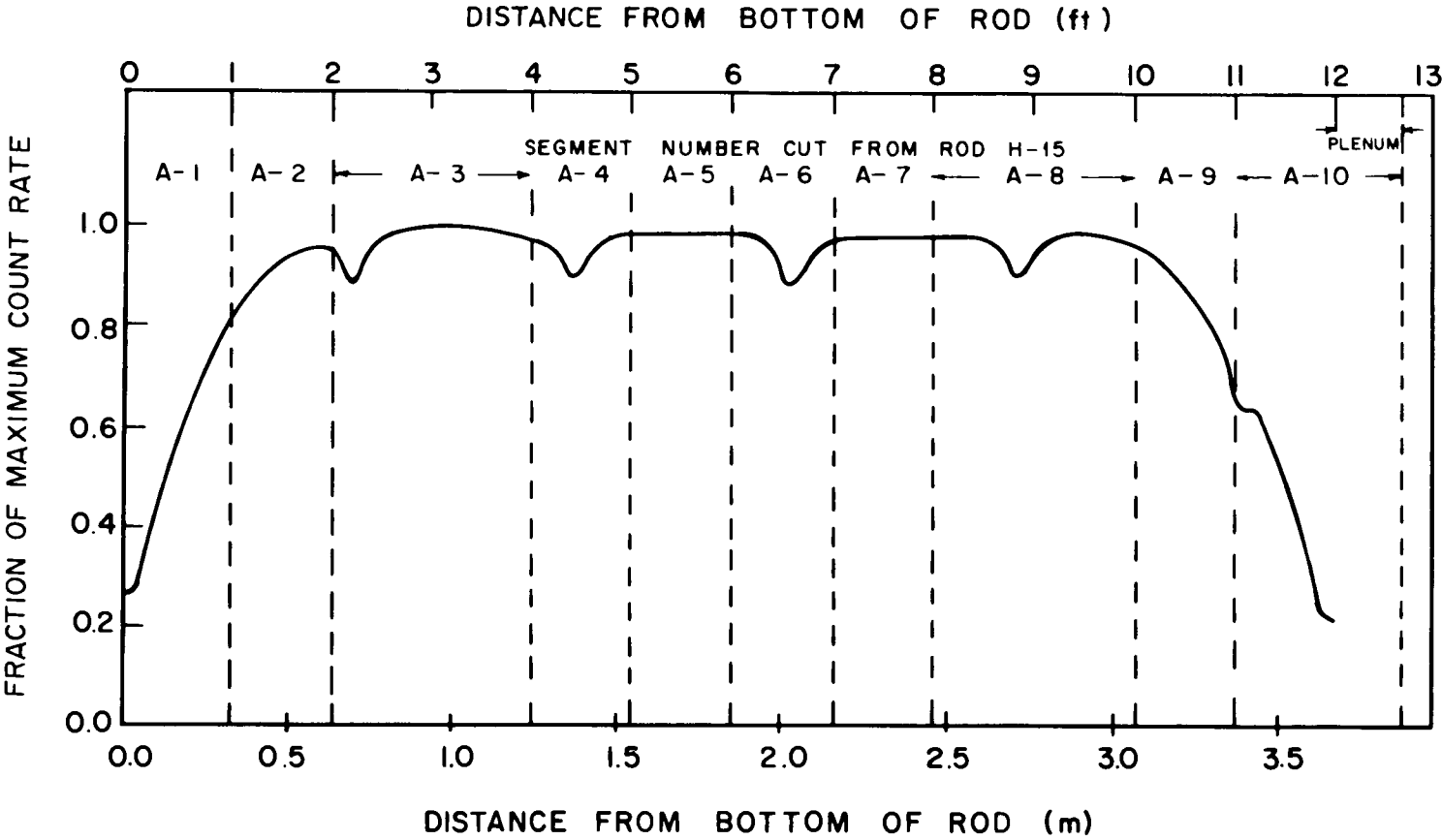


Fig. 1. Gamma profile of fuel rod H-15, showing locations of cuts; section A-8 was used in test HI-2.

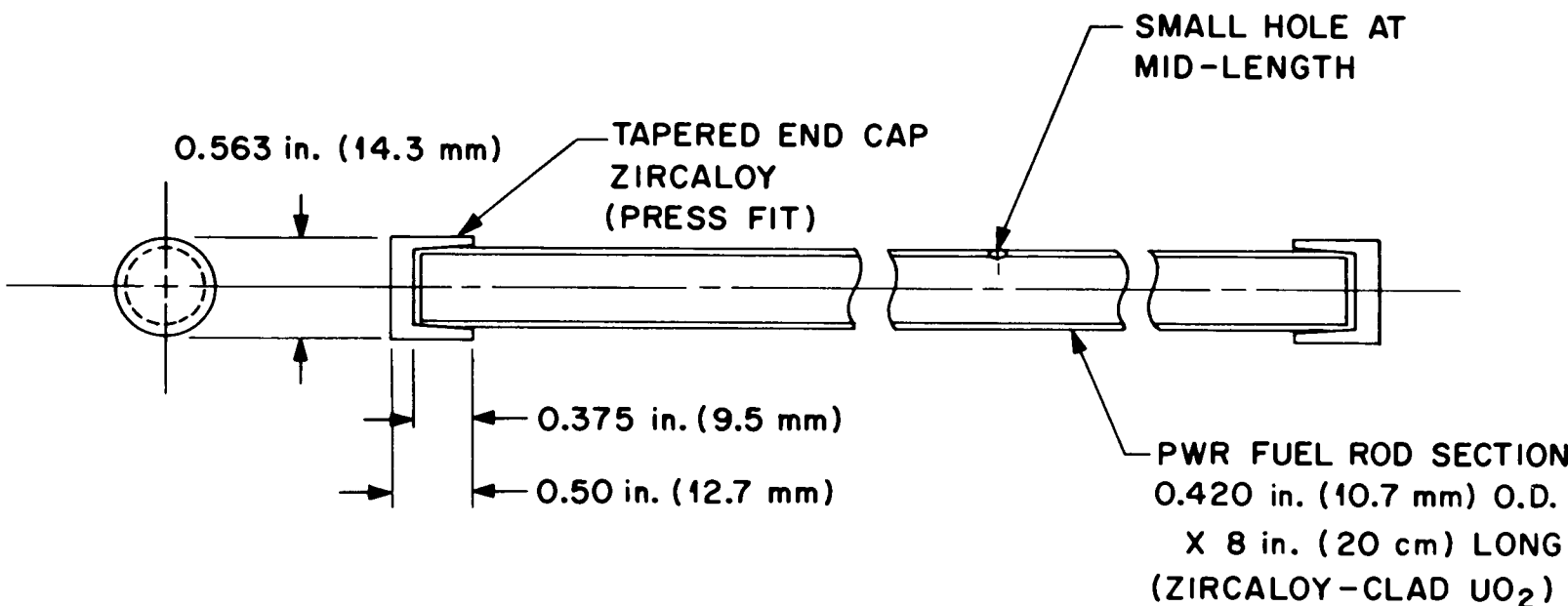


Fig. 2. Fuel specimen for fission product release studies.

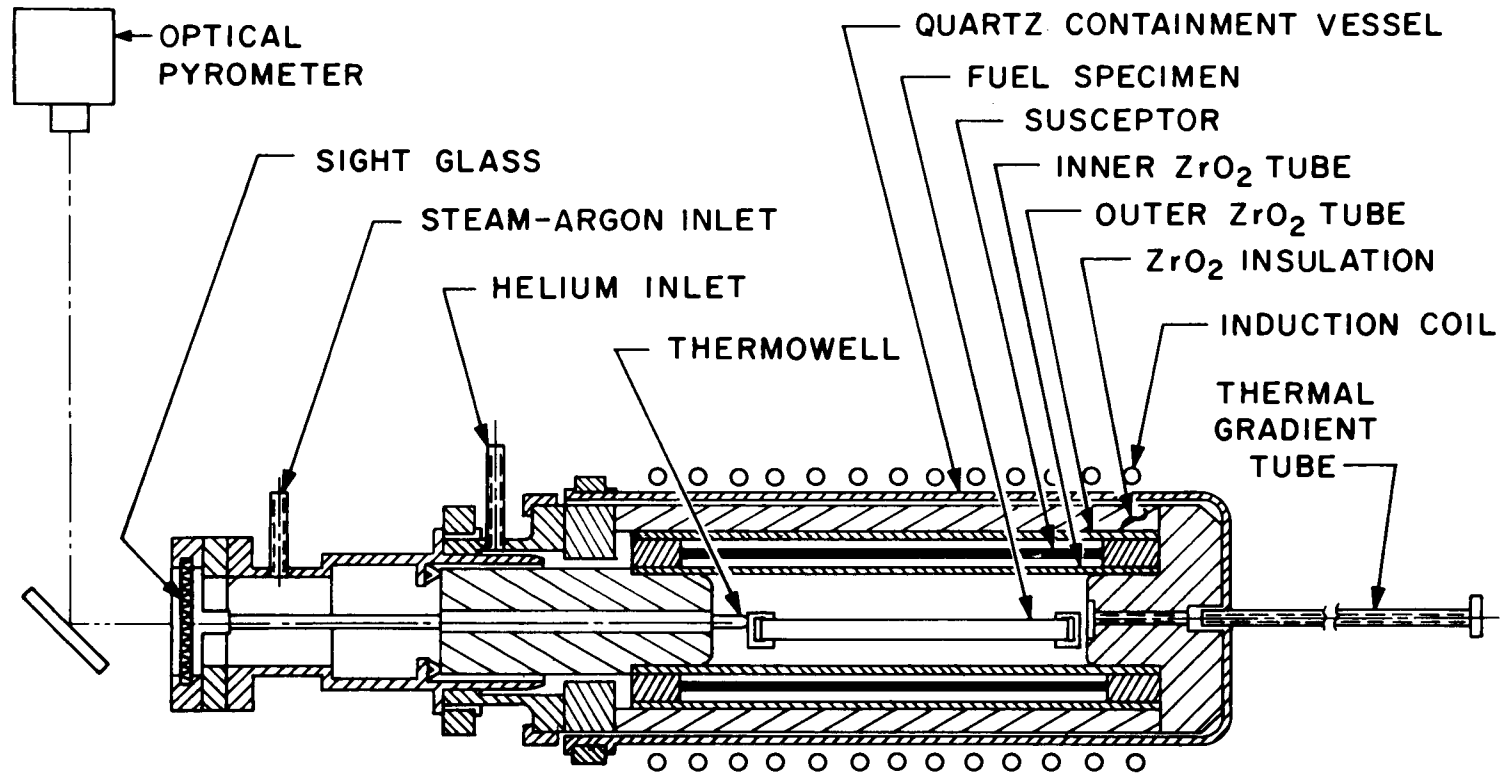


Fig. 3. Fission product release furnace.

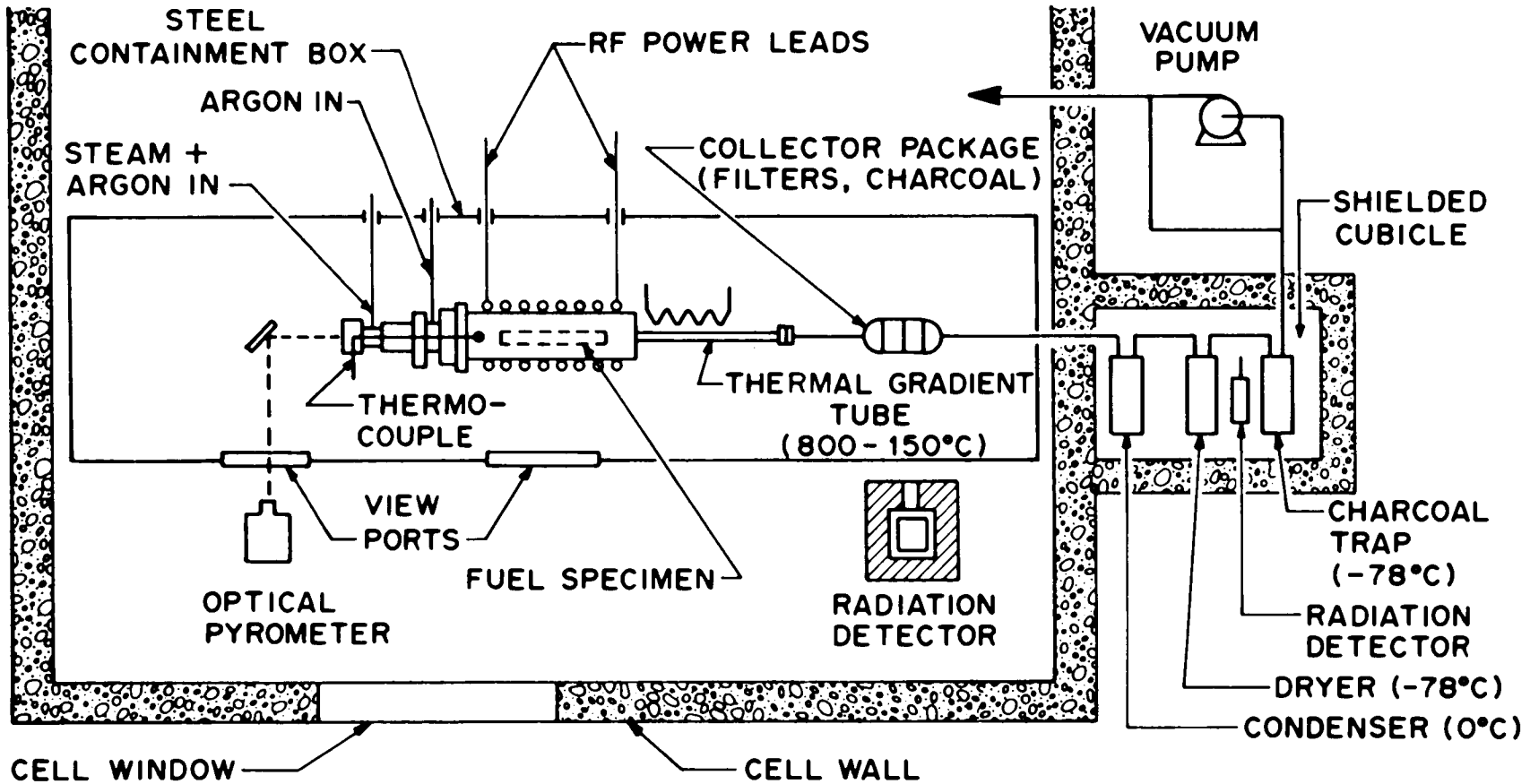


Fig. 4. Fission product release and collection system.

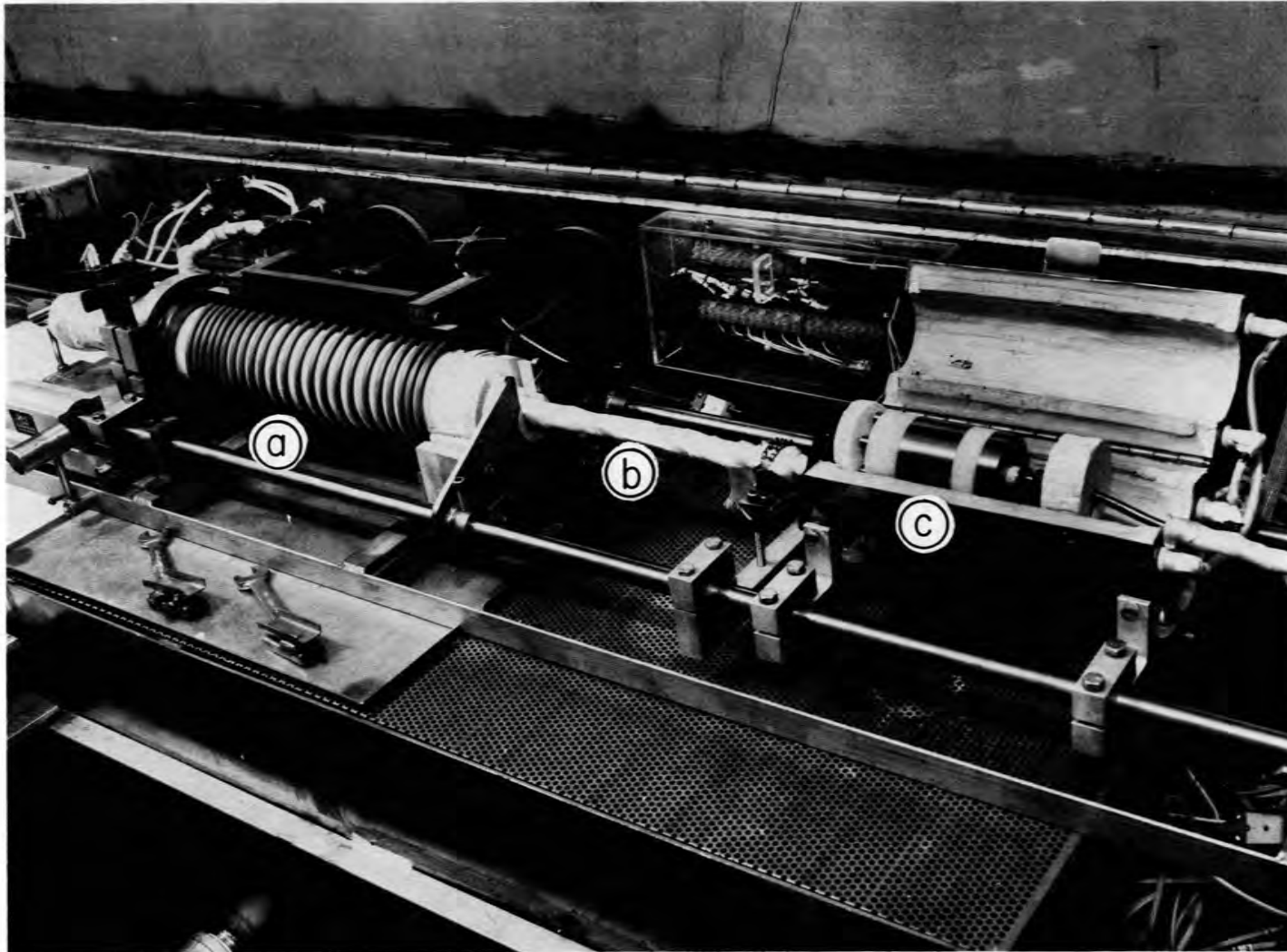


Fig. 5. Photograph of (a) fission product release furnace, (b) thermal gradient tube, and (c) filter package in steel containment box before test HI-2.

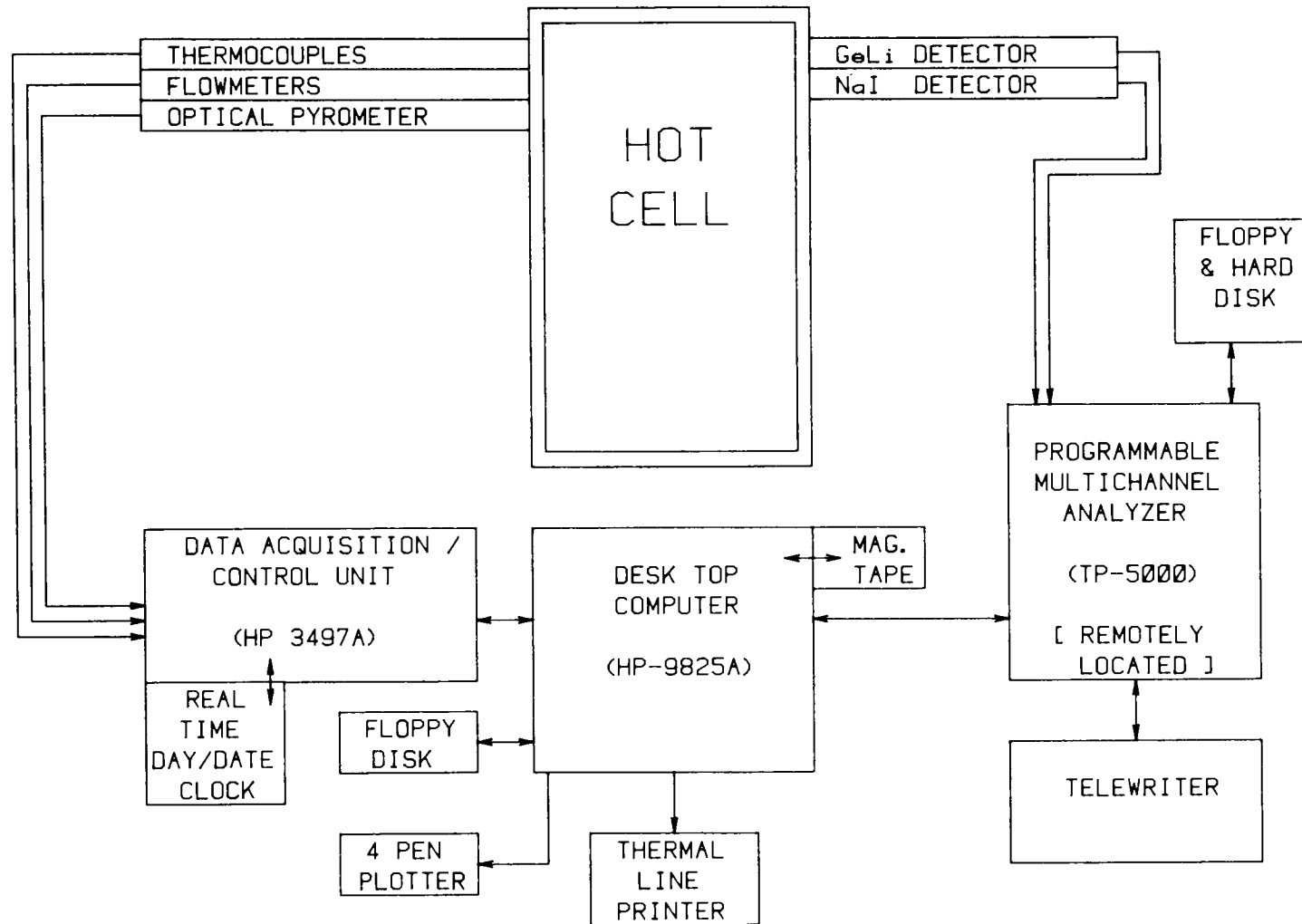


Fig. 6. Data acquisition and processing system for fission product release test.

Table 4. Operating conditions for test HI-2

Specimen temperature at start of heatup	280°C
Heatup rate	75°C/min
Nominal test temperature	1700°C
Time at test temperature	20 min
Nominal flow-rate data ^a	
Argon purge to tungsten susceptor	0.15 L/min
Argon to steam generator	0.30 L/min
Steam into system	1.0 L/min
Volume flow data ^b	
Argon purge	7.13 L
Argon to steam generator	14.22 L
H ₂ generated	13.54 L

^aAs measured by mass flowmeters.

^bAs measured by totalizers on mass flowmeters during the 64 min of steam flow into the apparatus.

well as for final closure of the furnace and containment box. No in-cell operations were required during the test.

2.4 Posttest Disassembly and Sample Collection

Following the high-temperature test and complete cooldown, the test apparatus was disassembled remotely. The filter package and thermal gradient tube liner were removed first and transferred to another hot cell to avoid potential contamination from fuel handling. The fuel specimen was then pulled from the furnace, inspected visually, photographed, and cast in epoxy resin in order to maintain its physical stability during handling. Thorough oxidation of the Zircaloy cladding during the test made it extremely fragile, and a continuous fracture that extended over about 80% of the length left the fuel pellets exposed. The appearance of the test specimen was similar to that of the unirradiated specimen shown at the top of Fig. 7. After the fuel specimen had been removed from the hot cell, personnel were allowed to enter the fuel handling area to carry out decontamination procedures. Then, the furnace was completely disassembled, and the components to be submitted for gamma-ray analysis were packaged. New, more complicated handling techniques were required since these components were typically about ten times more radioactive than those in test HI-1.

The filter package and the thermal gradient tube liner were too radioactive to permit direct gamma-ray spectrometry, even at a distance of 12 m. Therefore, these components were analyzed through 1 in. of lead, and the results were adjusted by energy-dependent attenuation factors. The liner of the thermal gradient tube was gamma-scanned at 1.3-cm (1/2-in.) intervals to determine the distribution of radioactivity (primarily ^{137}Cs) with temperature, then cut into seven sections based on this distribution. Smear samples from the liner were collected for mass spectrometric analysis. Each component of the liner and the filter package was analyzed by gamma spectrometry, before and after being leached successively with basic ($\text{NH}_4\text{OH} + \text{H}_2\text{O}_2$) and acidic ($\text{HNO}_3 + \text{HF}$) solutions. Iodine release values were obtained by activation analysis of both the solutions and the charcoal from the filter package.

3. TEST RESULTS

3.1 Test Data

The furnace was preheated in pure argon to about 300°C before steam flow through the system was begun. Heatup was started after the temperatures and steam flow had stabilized. The temperature and flow data for the test, presented in Fig. 8, are uncorrected; pretest temperature calibrations showed that the average temperature of the fuel specimen should have been 50 to 100°C above that indicated by the thermocouple and 100 to 150°C above the optical pyrometer values. The operating conditions for test HI-2 are summarized in Table 4. Based on the flow data, sufficient hydrogen was generated during the test (note the peak in total flow out at 15 to 20 min in Fig. 8) to account for greater than 90% oxidation of the Zircaloy cladding to ZrO_2 . Posttest examination confirmed

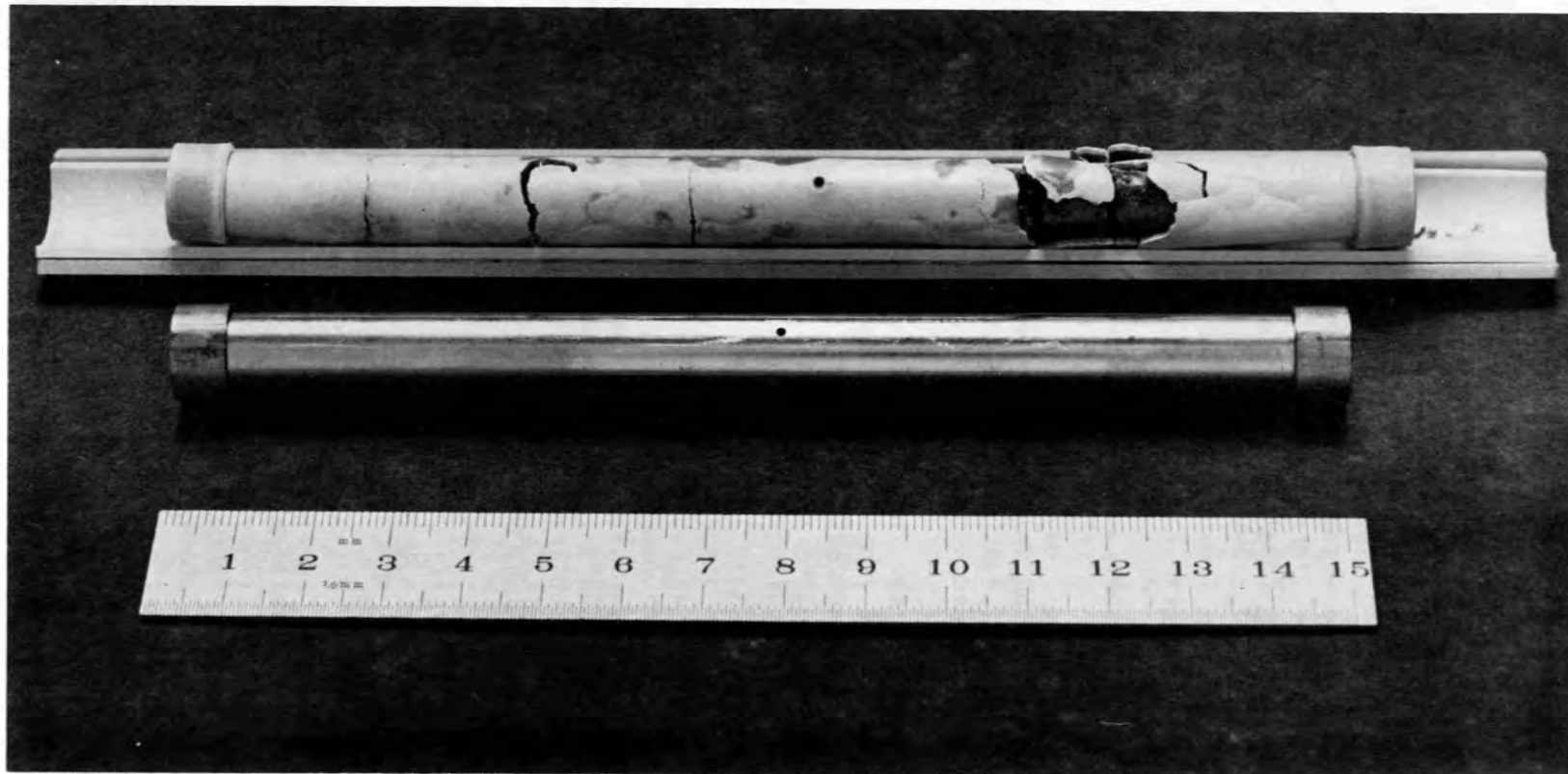


Fig. 7. Two unirradiated fuel specimens, illustrating the appearance before and after heating at 1700°C in steam.

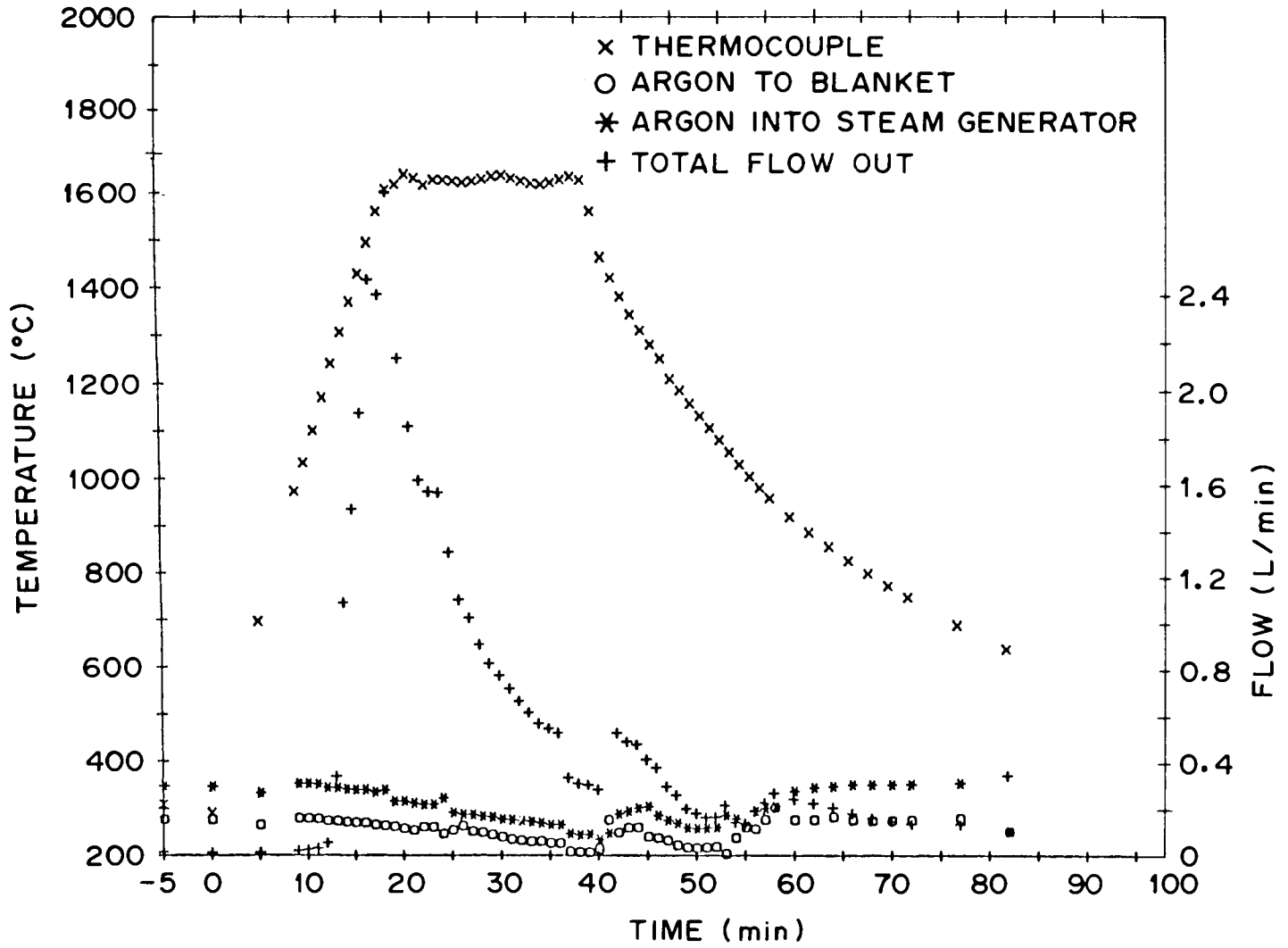


Fig. 8. Temperature and flow history of test HI-2.

this extensive oxidation. The release histories of ^{85}Kr to the cold charcoal traps and of ^{137}Cs to the thermal gradient tube and the filters are related to test temperature in Fig. 9. These values were determined as relative rates during the test, and quantitative measurements with a multichannel analyzer after the test were used to calculate fractional releases. The monitor for the thermal gradient tube viewed only the lower temperature end of the tube. Significant release during specimen cooling is apparent from the release curves.

3.2 Posttest Data

After the fuel specimen had been removed from the furnace, the test apparatus was disassembled and each component was counted by gamma-ray spectrometry to determine the amount of each gamma-radioactive species present. (As noted previously, ^{137}Cs and ^{134}Cs comprised most of the gamma activity in the fuel; these high levels of cesium interfered with analyses for the less abundant fission products.) The fractional release results for the various system components are summarized in Table 5.

3.2.1 Results from gamma spectrometry

The detailed results of gamma spectrometric analyses for ^{137}Cs , ^{125}Sb , and $^{110\text{m}}\text{Ag}$ are contained in Tables 6, 7, and 8, respectively. As expected, very little cesium was found on the highest-temperature components of the furnace (Table 6); most of it had migrated to regions where rapid condensation was possible. Approximately half of the cesium that escaped from the fuel was collected on the filters, indicating its association with particulate material. The distribution of cesium throughout the test apparatus is illustrated in Fig. 10; the iodine distribution, as determined by component leaching and activation analysis for ^{129}I , is included for comparison. These curves show the much higher levels of cesium as compared with iodine at most locations, reflecting the higher inventory of cesium (see Table 2). As in test HI-1, a high concentration of cesium occurred at the furnace outlet, indicating condensation (and possibly chemical reaction) on the ZrO_2 end plug at approximately 1300°C .

The basic solution that was used as a leachant to remove iodine from the test components also removed a large fraction of the cesium. As a result, the retained ^{125}Sb and $^{110\text{m}}\text{Ag}$ could be analyzed. The distribution of these elements (Cs, I, Sb, and Ag) along the thermal gradient tube is discussed in Sects. 3.2.4.1-3.2.4.4. The data for antimony and silver on all test components are summarized in Tables 7 and 8. It should be noted that these values represent minima; in several locations where the cesium concentrations were highest (e.g., the glass wool prefilter), no antimony or silver could be measured even though these elements were almost certainly present in significant quantities.

3.2.2 Results of activation analysis for iodine

Since iodine has no long-lived, gamma-emitting nuclides, analytical methods other than gamma spectrometry must be used. Neutron activation of

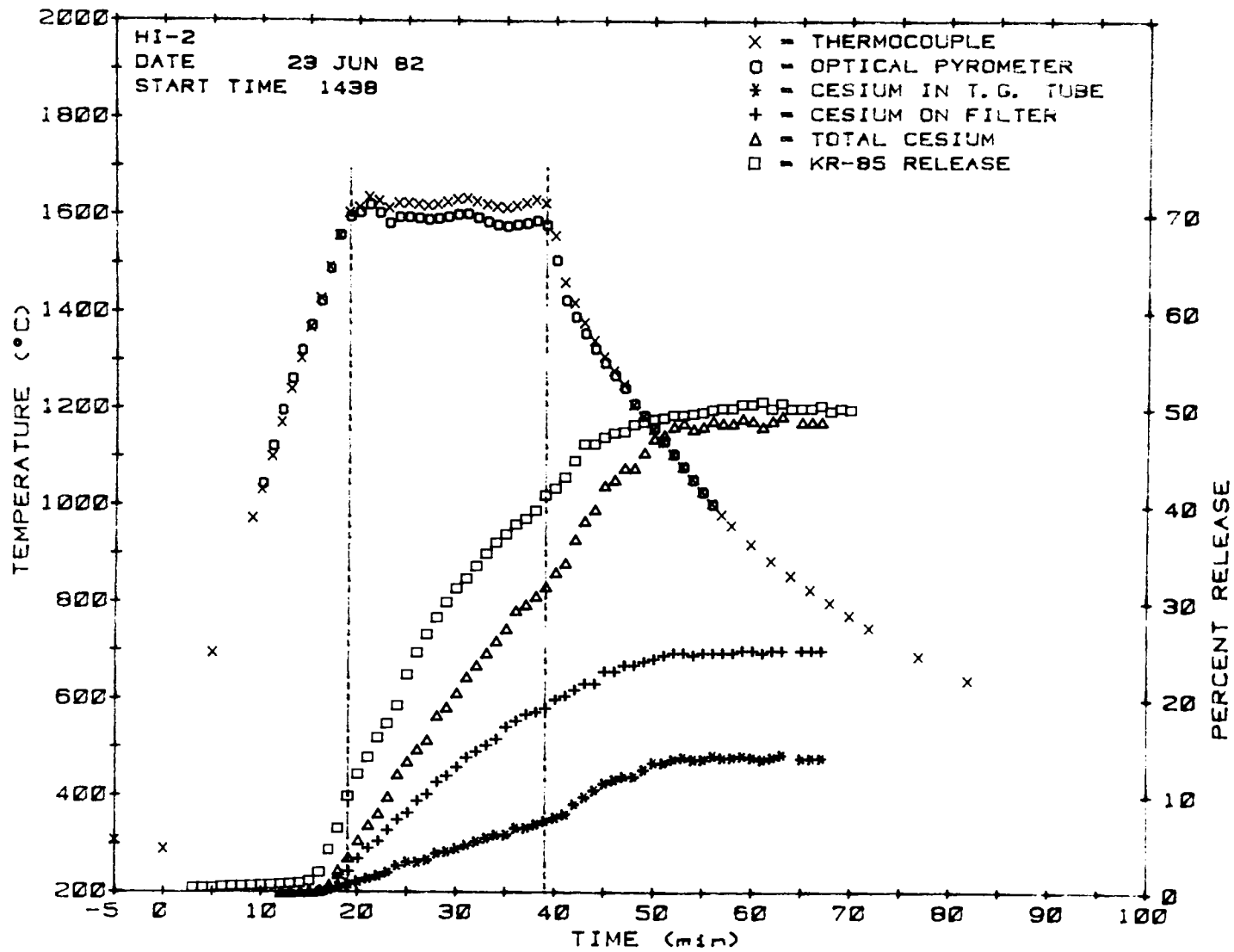


Fig. 9. Release of cesium and krypton as functions of time and temperature in test HI-2.

Table 5. Distribution of fission products released in test HI-2

Test component or collector	Temperature or range (°C)	Fraction of fuel inventory found (%)				
		⁸⁵ Kr	¹³⁷ Cs	¹²⁹ I	¹²⁵ Sb	^{110m} Ag
Furnace ^a	1700-1000	0	8.82	~0.14	0.68	0
Thermal gradient tube	1000-150	0	15.5	16.8	0.85 ^b	1.86 ^b
Filters	~150	0	26.2	35.9	0.005 ^c	0.26
Hot charcoal	~150	0	10 ⁻⁶	0.187	0	0
Cold charcoal	-78	51.5	0	0	0	0
Total		51.5	50.5	53.0	<1.53	2.12

^aIn addition, particles of fuel and/or cladding recovered from the furnace contained significant amounts of ¹³⁷Cs, ¹²⁵Sb, ¹⁰⁶Ru, and ⁶⁰Co.

^bMeasured only after more than 90% of the cesium activity had been removed by leaching.

^cNot detected on first filter because of high cesium activity (possibly as high as 0.1%).

Table 6. Distribution of cesium in test HI-2

Location	Temperature (°C)	Cesium found in each location		
		Amount (μ Ci 137 Cs) (mg total Cs)	% of specimen inventory ^a	% of total Cs released
Furnace components				
Inlet end components	~1000	2.479+1 ^b		
ZrO ₂ furnace tube	1700	2.534+1		
Tungsten susceptor	1800	4.807+1		
Outer ZrO ₂ tube	1700	3.535+2		
Fibrous ZrO ₂ insulator	~1200	7.807+2		
Outlet end components	~1200	1.504+5 ^c		
First ZrO ₂ outlet plug	1700	2.538+4		
Second ZrO ₂ outlet plug	1300	5.63+5		
Miscellaneous debris		7.131+3		
Quartz vessel	~800	1.60+4		
Total		7.88+5	21.95	8.82
Thermal gradient tube				
Quartz tube	~1000-140	1.027+5		
Segment 1	900-800	5.910+4		
Segment 2	800-700	8.550+4		
Segment 3	700-590	5.24+5 ^c		
Segment 4	590-460	2.081+5		
Segment 5	460-325	2.006+5		
Segment 6	325-220	1.218+5		
Segment 7	220-160	8.055+4		
Wipes from push rod		1.577+3		
Total		1.38+6	38.55	15.48
Filter package				
Entrance tube	~140	1.030+5		
Teflon entrance cone		4.283+4		
Glass wool prefilter		2.13+6 ^c		
First HEPA filter		6.735+4		
Second HEPA filter		4.706+0		
Heated charcoal		4.460-1		
Miscellaneous parts		4.106+2		
Total		2.34+6	65.18	26.18
Other components				
Condenser	0	5.66-2		
Cooled charcoal	-78	1.09-2		
Total		6.75-2	1.9-6	7.6-7
Total all components		4.51+6	125.7	50.48

^a Based on an average burnup of 28 MWd/kg, the test specimen contained 102.7 mg of 137 Cs (8.938 Ci) and 249.0 mg of total cesium. Inventory data were calculated by ORIGEN on May 24, 1982; the decay was corrected to July 15, 1981.

^b Exponential notation: 2.479+1 = 2.479×10^1 , 6.75-2 = 6.75×10^{-2} , etc.

^c Counted through 1-in. or 1.5-in. lead shielding because of high radioactivity.

Table 7. Distribution of antimony in test HI-2

Location	Temperature (°C)	Antimony found in each location			
		Amount		% of specimen inventory ^a	% of total Sb released
		(μ Ci ¹²⁵ Sb)	(μ g total Sb)		
Furnace components					
Quartz vessel	~800	91.32			
ZrO ₂ ceramics	1300-1700	1724			
Miscellaneous parts		4.48			
Total		1820	15.65	0.692	44.5
Thermal gradient tube					
Quartz tube (all)	~1000-140	ND ^b			
Segment 1	900-800	1529			
Segment 2	800-700	434.1			
Segment 3	700-590	230.2			
Segment 4	590-460	43.79			
Segment 5	460-325	13.79			
Segment 6	325-220	2.386			
Segment 7	220-160	1.884			
Total		2255	19.40	0.858	55.2
Filter package ~140					
Entrance tube		2.530			
Teflon entrance cone		0.818			
Glass wool prefilter		ND			
First HEPA filter		9.506			
Second HEPA filter		0.016			
Miscellaneous parts		0.016			
Total		12.88	0.111^c	0.0049	0.32
Total all components		4088	35.16	1.55	100

^aBased on an average burnup of 28 MWd/kg, the test specimen contained 0.255 mg of ¹²⁵Sb (262.9 mCi) and 2.262 mg of total antimony in the fuel; as a result of transmutation of antimony, the cladding contained 30.4 μ g of ¹²⁵Sb and 225 μ g of total antimony. Inventory data were calculated by ORIGEN on May 24, 1982; the decay was corrected to July 15, 1981.

^bND denotes not detected; in general, ¹²⁵Sb could not be detected before chemical removal of a large fraction of the cesium.

^cAdditional antimony was probably present (especially on glass wool prefilter) but could not be measured because of high levels of cesium radioactivity.

Table 8. Distribution of silver in test HI-2

Location	Temperature (°C)	Silver found in each location			
		Amount ($\mu\text{Ci } ^{110\text{m}}\text{Ag}$)	Amount ($\mu\text{g total Ag}$)	% of specimen inventory ^a	% of total Ag released
Furnace components					
Quartz vessel	~800	ND ^b			
ZrO ₂ ceramics	1300-1700	ND			
Thermal gradient tube					
Quartz tube	~1000-140	ND			
Segment 1	900-800	1.600			
Segment 2	800-700	1.502			
Segment 3	700-590	1.155			
Segment 4	590-460	1.249			
Segment 5	460-325	1.610			
Segment 6	325-220	0.495			
Segment 7	220-160	0.244			
Total		7.855	225.1	2.61	90.70
Filter package ~140					
Entrance tube		0.659			
Teflon entrance cone		ND			
Glass wool prefilter		ND			
First HEPA filter		0.146			
Second HEPA filter		ND			
Miscellaneous parts		0.001			
Total		0.806	23.09	0.268	9.30
Total all components		7.783	248.2 ^c	2.88	100

^aBased on an average burnup of 28 MWd/kg, the test specimen contained 6.3×10^{-5} mg of $^{110\text{m}}\text{Ag}$ (0.301 mCi) and 8.615 mg of total silver. Inventory data were calculated by ORIGEN on May 24, 1982; the decay was corrected to July 15, 1981.

^bND denotes not detected; in general, $^{110\text{m}}\text{Ag}$ could not be detected before chemical removal of a large fraction of the cesium.

^cAdditional silver was probably present but could not be measured because of high levels of cesium radioactivity.

ORNL DWG 83-139

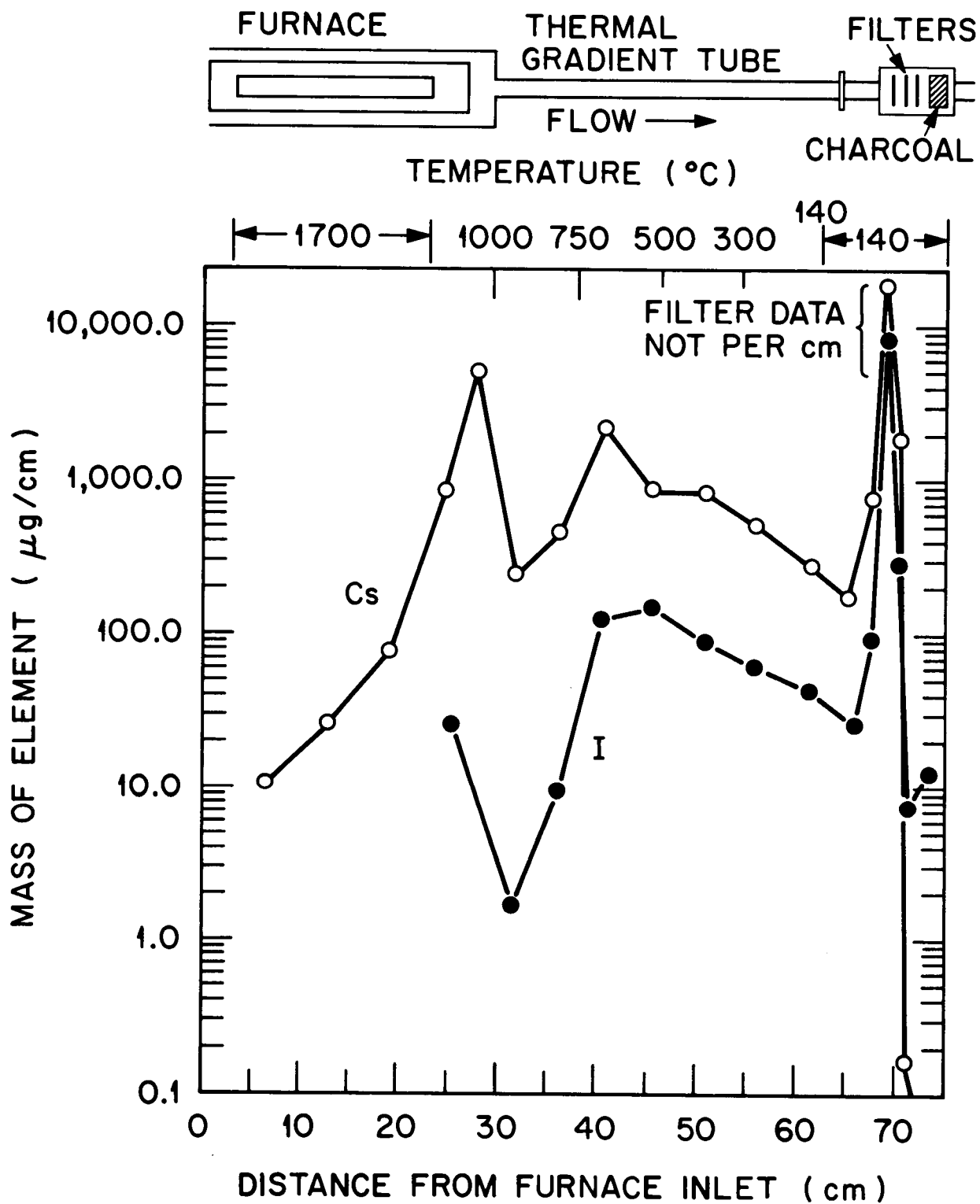


Fig. 10. Distribution of fission products in test HI-2.

^{129}I to ^{130}I , which can be counted easily, is a proven, sensitive technique. Iodine forms dissolve readily in basic solutions to form stable iodides; in our samples, large amounts of highly radioactive cesium were also dissolved. Small aliquots of the solutions were chemically treated to remove cesium prior to being irradiated; then the 12.4-h ^{130}I was counted. The results of these analyses, along with the data on fractional iodine release and the cesium/iodine ratios at various apparatus locations, are summarized in Table 9. The very low cesium/iodine ratios on the second HEPA filter, the heated charcoal, and the condenser show that a very small fraction ($<0.054\%$) of the iodine was of a form that penetrated the first two filters. The total fraction of iodine released, 53.79%, is actually a minimum value since iodine cannot be detected directly and it is not possible to leach and sample all surfaces of the test apparatus. The total amount of iodine found, however, is in good agreement with the amounts of krypton and cesium (Table 5), thus indicating that no significant amount of the released iodine was missed.

3.2.3 Results of spark-source mass spectrometric analyses

Spark-source mass spectrometry (SSMS) was used to obtain elemental analyses of (1) smear samples from two areas of the thermal gradient tube and the glass wool prefilter, and (2) solution samples from the same components and from the ZrO_2 furnace ceramics. Either the amount of ^{137}Cs , as measured by gamma spectrometry, or a known quantity of erbium added as a standard was used to determine mass values for the fission product, structural, and impurity elements detected. Although these values were not highly precise (an accuracy of a factor of 2 is claimed for the analysis, and perhaps a similar uncertainty is associated with the sampling method), we did obtain data for several important elements that were not otherwise available.

The results of all the SSMS analyses are summarized in Table 10. The data from solution samples include both the basic and the acidic leaches; however, it should be noted that all of the chemical forms present on the test components were not necessarily soluble in either leach solution. Consequently, the smear samples should supply more representative results than those obtained for the solution samples.

For those elements where comparisons are possible (i.e., Cs, I, and Ag), the SSMS data agree reasonably well with the gamma spectrometry data. The SSMS values obtained for solutions are generally lower than those for smears; this is apparent in the comparison of smear and solution values from the glass wool prefilter. Surprisingly large amounts of tellurium, about three times the amount of cesium, were indicated for sections 3 and 4 of the thermal gradient tube. Similarly, the relatively large amounts of silver found on the same samples cannot be explained. Of the non-fission-product elements, the larger amount (272 mg) of tungsten from the susceptor found in the prefilter solution, without being detected on the smear, appears to be an anomaly. We believe that the high sensitivity of this measurement technique, combined with the inherent problems of

Table 9. Distribution of iodine in test HI-2
(Results of activation analysis for ^{129}I)

Location	Temperature (°C)	Iodine found in each location				Cs/I ratio ($\mu\text{g Cs}/\mu\text{g I}$)
		Amount ($\mu\text{g } ^{129}\text{I}$)	Amount (mg total I)	% of specimen inventory ^a	% of total I released	
Furnace components						
Quartz vessel	~800	493				0.685
ZrO ₂ ceramics	1300-1700	26.7				466
Total		520	0.687	2.77	5.14	31.9
Thermal gradient tube						
Quartz tube (all)	~1000-140	972				2.23
Segment 1	900-800	6.77				184
Segment 2	800-700	26.4				68.3
Segment 3	700-590	444				24.9
Segment 4	590-460	523				8.40
Segment 5	460-325	341				12.42
Segment 6	325-220	232				11.09
Segment 7	220-160	157				10.84
Total		2702	3.568	14.37	26.71	10.80
Filter package ~140						
Entrance tube		326				6.67
Teflon entrance cone		108				8.34
Glass wool prefilter		6195				7.25
First HEPA filter		210				6.77
Second HEPA filter		5.3				0.019
Heated charcoal 1		18				0.00025
Heated charcoal 2		6.6				
Heated charcoal 3		5.8				
Heated charcoal 4		6.4				
Miscellaneous parts		9.2				0.909
Total		6890	9.095 ^b	36.63	68.12	7.17
Condenser	0	3.08	0.0041	0.017	0.03	0.00039
Total all components		10,115	13.354	53.79	100	9.41

^aBased on an average burnup of 28 MWd/kg, the test specimen contained 18.80 mg of ^{129}I and 24.83 mg of total iodine. Inventory calculations were made by ORIGEN on May 24, 1982; the decay was corrected to July 15, 1981.

^bIn addition, 3.9 μg of bromine was found on the charcoal; this value corresponds to 0.18% of the specimen inventory as compared with 0.20% of the iodine found on the charcoal.

Table 10. Results of spark-source mass spectrometry^a of samples from test HI-2 components

Element	Mass of element found (mg)					
	Thermal gradient tube			Glass wool prefilter		ZrO ₂ ceramics
	Sect. 1 _b (Smear) ^b	Sect. 3 (Solution) ^c	Sect. 4 (Smear)	(Smear)	(Solution)	(Solution)
Fission products						
Cs (R) ^d	1.20	2.2	4.33	53.5	29.4	1.1
Rb (R)	0.24	0.40	0.87	11.0	5.8	0.45
I (R)		0.29	3.0	5.7	5.0	<0.9
Br			0.04			
Te	0.12 (R)	7.7 (R)	13 (R)	~27	5.9 (R)	
Cd	<0.006 (?)	0.27 (R)	1.7 (R)	5.0 (?)	1.5 (N)	<0.2
Ag	0.064 (R)	0.35 (N)	0.009 (R)	4.8 (R)	0.013 (N)	0.11 (N)
Mo (R)	6.0	0.18	0.43	10.7	6.1	0.67
Ru						0.67
Se (R)	0.06		0.22			
Special materials						
Pt						
Sn (N)	0.36	2.3	3.9	27	6.4	
Zr (N)		0.025	0.002	0.54	0.019	
Au			1.3			
Other materials						
Hg		0.25			14	2.2
Bi		0.16		1.6	0.32	
Pb		0.22		1.1	0.32	
Ta				48 (?)	<4.1	<11
Re					11	2
W					272	45
Fe	0.01	0.13		0.4	1.0	6.7
Mn		0.003			<0.15	0.11
Total deposit - all materials	~10	~15	~29	~230		

^aPrecision is plus or minus a factor of 2.

^bData based on gamma analysis for cesium.

^cData based on erbium tracer added to sample.

^d(R) denotes radiogenic isotopic distribution, (N) denotes natural isotopic distribution, and (?) denotes mixture or uncertain.

collecting samples in the hot cell, may lead to a number of element identifications that are not relevant to the fission product release test itself but, instead, are artifacts of posttest sample collection and handling.

3.2.4 Thermal gradient tube results

The thermal gradient tube is made of quartz, 36 cm long and 0.4 cm in internal diameter, and lined with platinum foil. Its temperature was controlled by two independent heaters, each with a coil spacing that varied along its length. The aim was to produce a linear gradient in temperature from gas inlet to gas outlet. Fifteen thermocouples were used to monitor the temperature of the outside surface of the quartz tube and to control the temperature manually. The temperature profile changed slightly during the experiment as the enthalpy of the flowing gas varied. Figure 11 shows the average temperature profile measured during test HI-2; the temperature of the platinum deposition surface was greater by an unknown amount.

After the test, the platinum liner was removed and gamma counted through a 0.635-cm (0.25-in.) slit at 1.27-cm (0.5-in.) intervals. Cesium-134 and ^{137}Cs dominated the counting, as shown by the profile presented in Fig. 12. Because this detector was uncalibrated in this geometry, the profile has been scaled so that 1.28 Ci of ^{137}Cs is present in the total; this figure was obtained by a calibrated count of the entire liner. The activity was converted to the amount of cesium (all isotopes), using the factor $1 \mu\text{Ci of } ^{137}\text{Cs} = 2.786 \times 10^{-2} \mu\text{g of Cs}$, which was derived from an ORIGEN calculation.

The platinum liner was cut into seven sections, as shown in Fig. 11, using the ^{137}Cs profile to guide the cuts. Each section was counted, leached with $\text{NH}_4\text{OH}/\text{H}_2\text{O}_2$, recounted, leached with $\text{HNO}_3 + \text{HF}$, and counted a third time. Table 11 shows the results. The cutting operations dislodged 24% of the cesium activity; only 0.9668 Ci was present afterward. The leaching processes removed most of the cesium, and ^{125}Sb and $^{110\text{m}}\text{Ag}$ peaks were revealed. In cases where data are available, they show that neither the basic nor the acidic leach affected the antimony or silver deposits. The seven basic leach solutions were analyzed for ^{129}I by neutron activation. Table 12 collates the results for ^{137}Cs , ^{129}I , $^{110\text{m}}\text{Ag}$, and ^{125}Sb ; the elemental totals are plotted in Figs. 12, 13, 14, and 15, respectively.

3.2.4.1 Cesium on the thermal gradient tube

The cesium profile in Fig. 12 consists of a large doublet peak between 520 and 730°C and three smaller peaks centered at 900, 800, and 400°C.

Cesium in the irradiated fuel is present in great excess over electronegative fission products (tenfold excess over iodine, the most abundant); thus, the bulk must be transported as oxide or hydroxide species in the steam atmosphere. The large doublet peak probably represents some

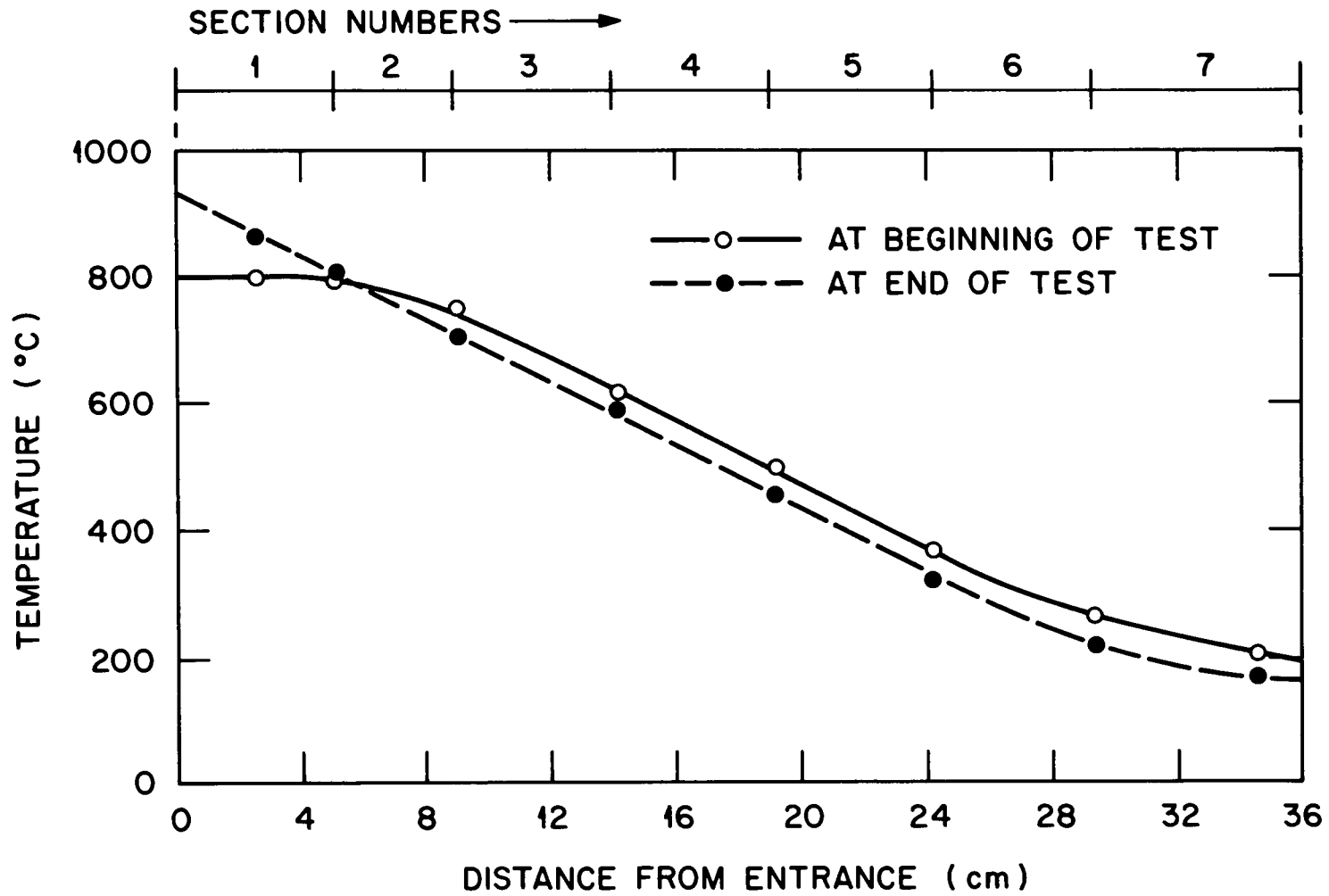


Fig. 11. Temperature distribution along thermal gradient tube, test HI-2.

ORNL DWG 82-1486

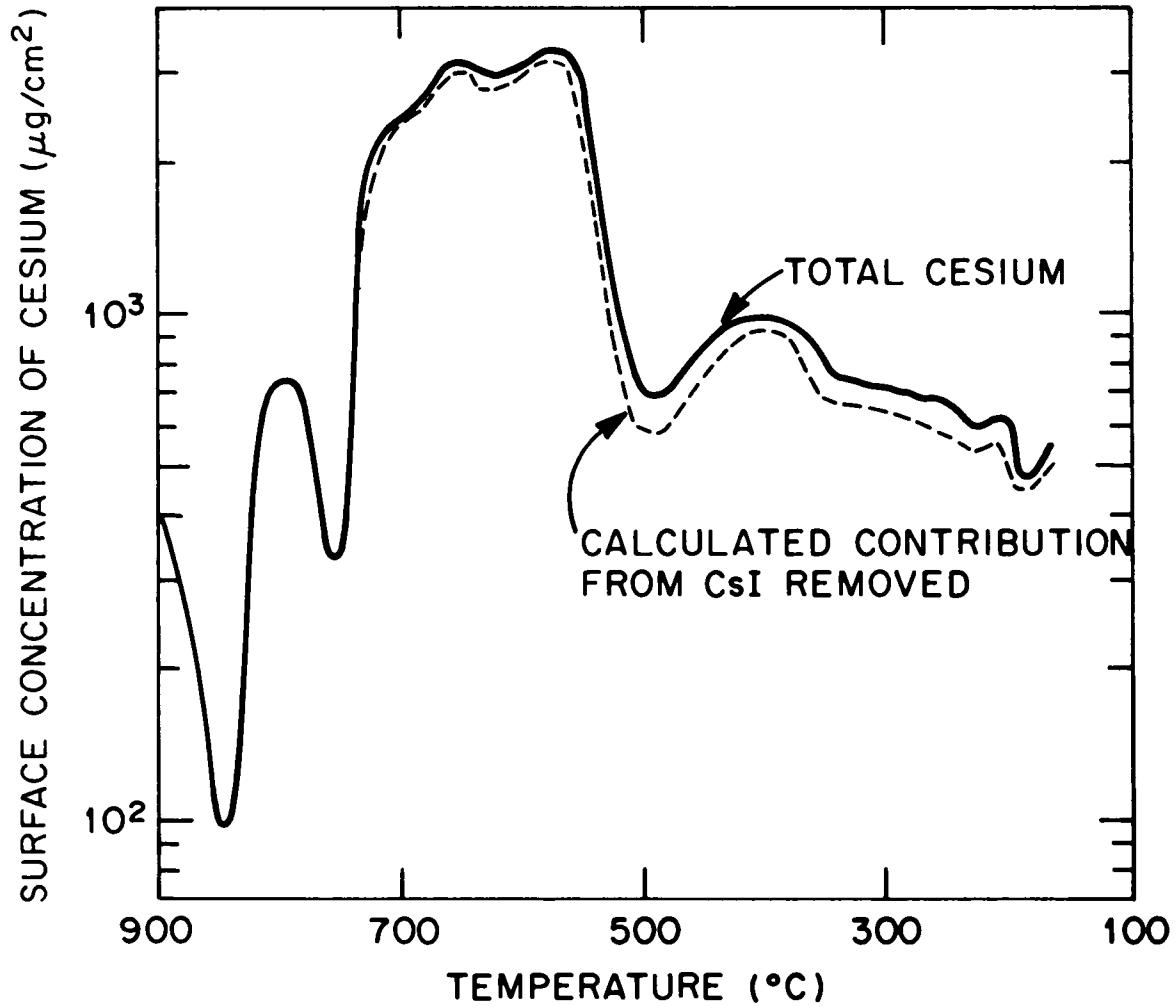


Fig. 12. Mass of cesium in thermal gradient tube after test HI-2.

Table 11. Fission products on thermal gradient tube sections before and after leaching

Section No.	Length (cm)	Concentration of element ^a (μg/cm)							
		Before leaching		After basic leach			After acid leach		
		Cs	Sb	Cs	Sb	Ag	Cs	Sb	Ag
1	5.1	2.45+2 ^b	2.21	7.62	2.59	9.02	4.99	2.36	1.13+1
2	3.8	4.72+2	0.907	4.12+1	9.80-1	11.30	3.28+1	9.30-1	ND
3	5.1	2.17+3	ND ^c	3.64+1	3.90-1	6.51	1.19+1	3.15-1	ND
4	5.1	8.62+2	ND	2.59	7.4-2	7.04	1.40	6.8-2	6.90
5	5.1	8.31+1	ND	1.19	2.3-2	9.09	5.22-1	1.7-2	7.22
6	5.1	5.04+2	ND	7.68-1	4.0-3	2.80	2.75-1	6.7-4	6.99-1
7	6.3	2.67+2	ND	7.82-1	2.6-3	1.10	2.42-1	5.3-4	2.93-1

^a Based on ¹³⁷Cs, ¹²⁵Sb, and ^{110m}Ag.

^b Exponential notation: 2.45+2 = 2.45 × 10², etc.

^c ND denotes not detected; no ^{110m}Ag was detected before the basic leach.

Table 12. Fission products on HI-2 thermal gradient tube

Position (cm)	Temperature range (°C)	^{137}Cs ^a (μCi)	Cesium ($\mu\text{g}/\text{cm}^2$)	^{129}I ^b (μg)	Iodine ($\mu\text{g}/\text{cm}^2$)	$^{110\text{m}}\text{Ag}$ ^c (μCi)	Silver ($\mu\text{g}/\text{cm}^2$)	^{125}Sb ^c (μCi)	Antimony ($\mu\text{g}/\text{cm}^2$)
0-5.1	900-800	$4.5+4$ ^d	2.6+2	6.77	1.4	1.6	9.6	1.5+3	2.7
5.1-8.9	800-700	6.5+4	5.0+2	26.4	7.3	1.5	12.0	4.3+2	1.0
8.9-14.0	700-590	4.0+5	2.3+3	444	92	1.2	6.9	2.3+2	4.1-1
14.0-19.1	590-460	1.6+5	9.1+2	523	110	1.2	7.5	4.4+1	7.9-2
19.1-24.1	460-325	1.5+5	8.8+2	341	71	1.6	9.6	1.4+1	2.5-2
24.1-29.2	325-220	9.2+4	5.4+2	232	48	0.50	3.0	2.4	4.3-3
29.2-35.6	220-160	6.1+4	2.8+2	157	32	0.24	1.2	1.9	2.7-3

^aOn specimens before leach.

^bBy neutron activation analysis to ^{130}I .

^cMeasured after basic leach; ^{137}Cs dominates the activity before basic leach.

^dExponential notation: $4.5+4 = 4.5 \times 10^4$, $2.7-3 = 2.7 \times 10^{-3}$, etc.

ORNL DWG 82-1485

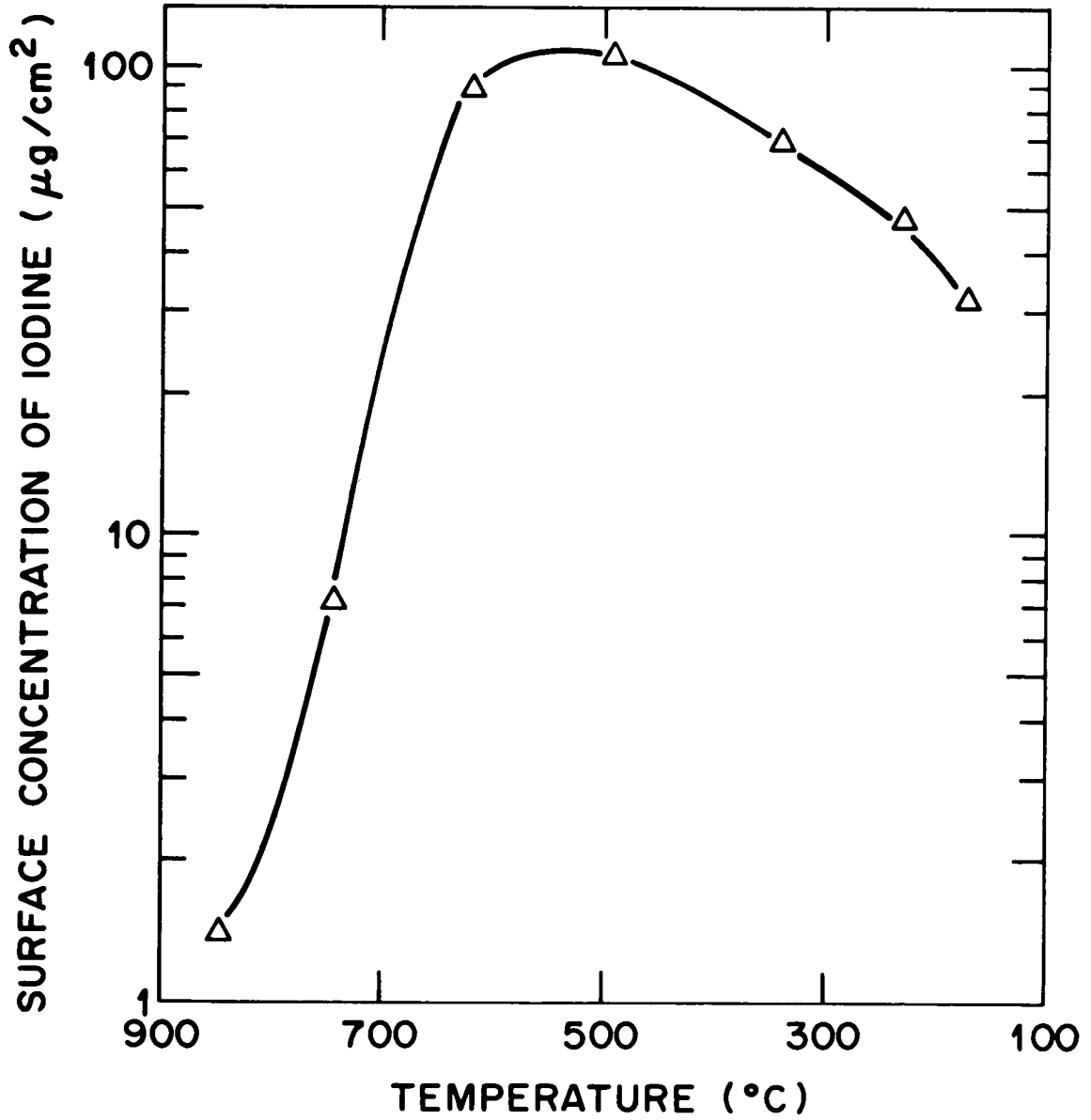


Fig. 13. Mass of iodine in thermal gradient tube after test HI-2.

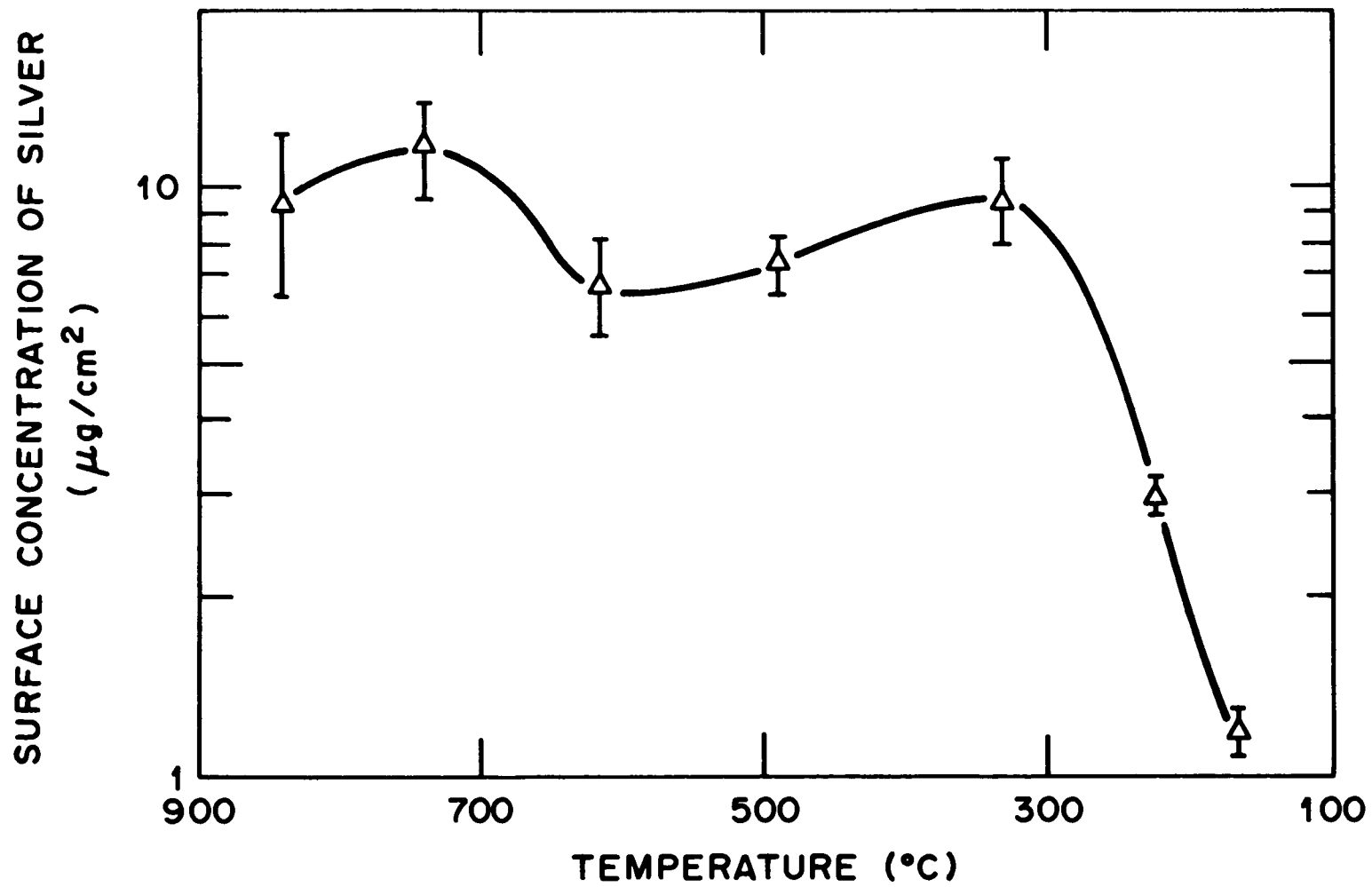


Fig. 14. Mass of silver on thermal gradient tube after test HI-2.

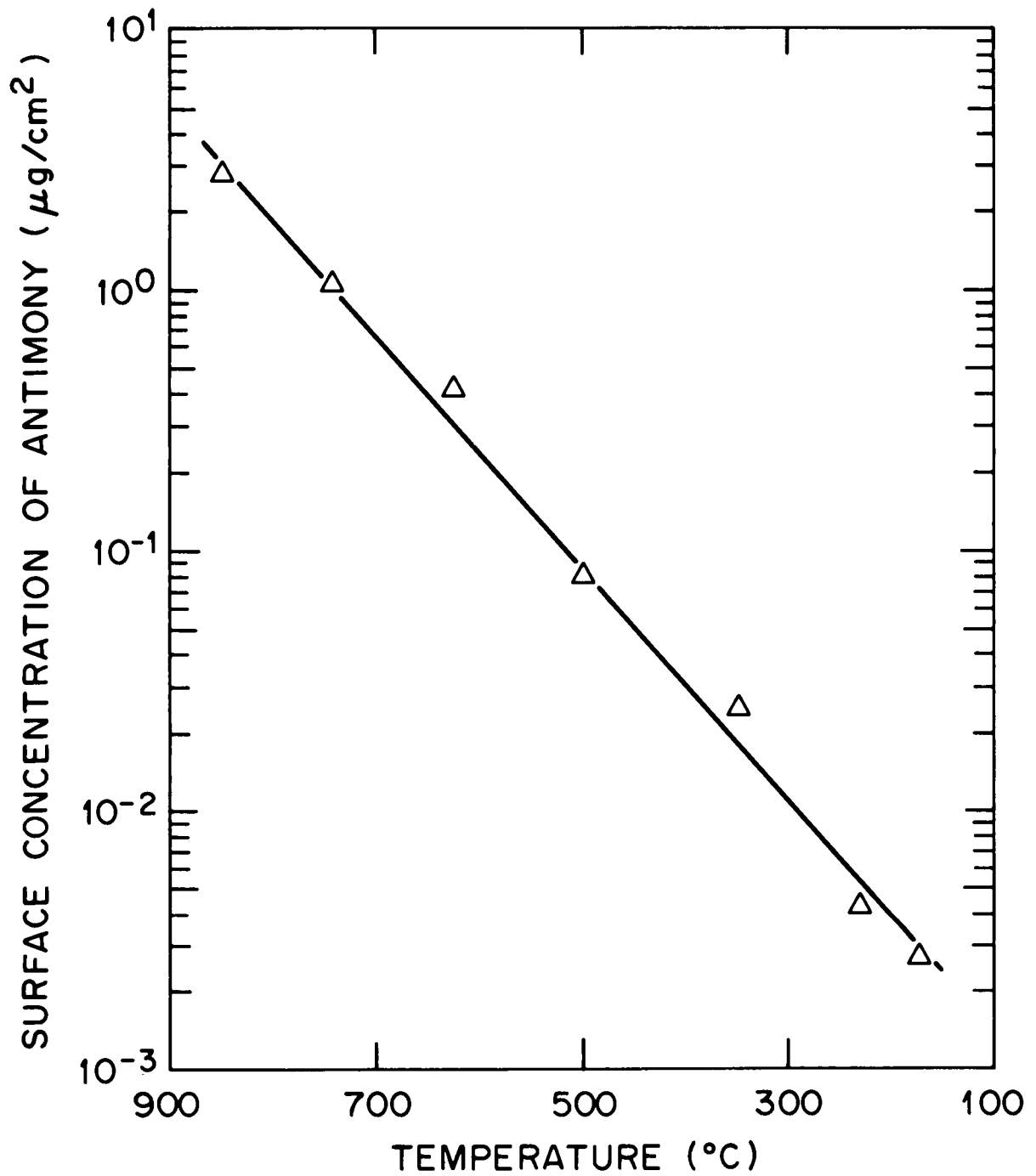


Fig. 15. Mass of antimony in thermal gradient tube after test HI-2.

such species, although CsOH should not deposit above 510°C under the conditions of test HI-2. This peak, as well as the two small peaks centered at 800 and 400°C, may reflect Cs-O compounds containing tungsten (from the induction furnace susceptor), molybdenum (fission product), or zirconium (from fuel cladding). Significant amounts of these elements have been found on the thermal gradient tubes in both tests, HI-1 and HI-2, by SSMS.

The peak at the inlet to the thermal gradient tube, centered at 900°C, was probably caused by fuel and ZrO₂ dust settling at a location where the gas flow was disturbed.

None of the cesium peaks corresponds to pure CsI. We have calculated the maximum contribution to the cesium profile from CsI and subtracted it, as shown in Fig. 12. Since the cesium profile was almost unchanged, we can assume that the presence of iodine did not affect the deposition of cesium.

Sixty-four percent of the cesium entering the thermal gradient tube escaped to be collected on the filters. It may have been present as aerosol, or else the gas in the tube remained much hotter than the platinum liner and cesium compounds remained volatile.

3.2.4.2 Iodine on the thermal gradient tube

The iodine profile (Fig. 13) is characterized by a steep rise to a peak at 600 to 500°C followed by a gentle decrease. This behavior is typical of a compound that can be adsorbed on platinum and then be desorbed again by a thermally activated process, such as condensation of a vapor to a solid. As the temperature decreased from 800°C to 600°C, the iodine compound adsorbed; however, desorption occurred less and less readily as the profile rose. Around the 600°C position, the iodine compound began to vanish from the gas phase and the profile dropped to the outlet end of the tube.

If all the iodine was present as CsI and was released at a constant rate during test HI-2, the peak should start where the gas became supersaturated in CsI vapor. This temperature lies in the range 600 to 700°C, depending on the source of CsI vapor pressure data.

The profile drops by a factor of 3 from its peak to the outlet. The profile is affected by the decrease in gas-phase concentration with length and by the decreasing diffusion coefficient with temperature (hence length). The former can account for a profile drop factor of 1.47 and the latter a factor of up to 7. This is good agreement with the observed factor of 3 since the exact figures depend on the detailed temperature and velocity gradients in the gas, both of which are unknown.

The 68% of the iodine that escaped the thermal gradient tube was adsorbed on the filters at 150°C; only 0.4% penetrated the filters. This is typical behavior for an aerosol, but not for molecular iodine.

Iodine behavior was consistent with its transport as CsI vapor and aerosol, with a negligible contribution from molecular iodine.

3.2.4.3 Silver on the thermal gradient tube

We can draw only very tentative conclusions from the silver profile shown in Fig. 14. There are apparently two species, one of which has a monotonically decreasing profile similar to antimony and may be elemental silver. Superimposed on this is a broad peak centered at 320°C, typical of a compound which may be AgI or Ag₂Te. These compounds are easily decomposed by reducing conditions and heat, respectively.

3.2.4.4 Antimony on the thermal gradient tube

The behavior of antimony on the thermal gradient tube (Fig. 15) may be explained as elemental antimony reacting rapidly and irreversibly with the platinum surface of the tube in such a manner that gas-phase diffusion of antimony molecules limits the rate. In this case, the profile should follow the gas-phase concentration of antimony and the value of the gas-phase diffusion coefficient.

Antimony will probably be released from the fuel in the elemental form. The oxides are not stable to reduction,¹⁰ and noble metal-antimony alloys should decompose to produce antimony vapor. Antimony alloys with platinum to form a number of compounds such as PtSb, PtSb₂, and Pt₄Sb.¹¹ In addition, it forms a solid solution below 10 at. % antimony. This provided an opportunity for irreversible reaction with the platinum surface and explains why neither basic nor acidic leaches removed it from the thermal gradient tube.

According to our data, the surface concentration of antimony decreased by a factor of 1000 along the thermal gradient tube. Based on the amount of antimony collected on the filters, the gas-phase concentration decreased by a factor of 170. The temperature dependence of the gas-phase diffusion coefficient added another factor of up to 9, making the total factor less than 1500. The agreement between 1000 and <1500 corroborates the explanation of antimony behavior.

If antimony was released at a constant rate during the test, it would have entered the thermal gradient tube at a pressure of 1.0 mPa. At 850°C, the vapor pressure of pure antimony is about 0.3 kPa; thus, antimony must have diffused into the platinum during the test sufficiently rapidly to reduce its activity below 0.003% of the activity of the element. This required the antimony to alloy evenly to a depth of 7 μm during the 20-min duration of the test, which is certainly possible if antimony diffuses as rapidly in platinum as it does in silver.

3.2.5 Results of analysis of cladding and end-cap samples from tests HI-1 and HI-2

The H. B. Robinson fuel used in tests HI-1 and HI-2 was clad in Zircaloy that contained about 1.5% tin. The tin was activated during irradiation in the reactor; at the time we tested the fuel in HI-2, this tin activity had almost completely decayed to ^{125}Sb . In addition, fission products from the fuel had attached themselves to the Zircaloy by recoil, diffusion into it, or adsorption on its surface. The fuel specimen was cut to length from a fuel rod, and new, unirradiated Zircaloy end caps were fitted over the open ends.

Following test HI-2, the samples of cladding and downstream end cap were separated and analyzed by gamma spectrometry. Any difference between the cladding and the end cap should reflect the behavior of the fission products. The cladding and end-cap samples were placed in clean glass bottles and counted. Then the epoxy resin mounting material was removed, and the samples were rinsed in distilled water and counted separately. Minimal activity was lost during the separation and rinsing procedures; the extreme value was 11% for ^{60}Co .

Similar specimens from test HI-1 were prepared and treated in the same way. In this case, however, about 20 to 40% of the fission products were lost in handling.

3.2.5.1 Interpretation

This section discusses test results from both HI-1 and HI-2 because each influences the other. Tables 13 and 14 summarize the results.

The fission products present on the cladding and end caps reached those locations by traveling with fine fuel particles or as individual nuclides in the vapor phase. The second mechanism reflects the chemical species present and, therefore, is more interesting.

Cerium-144 was chosen as a fuel marker because it was present as an involatile oxide under the reducing conditions of tests HI-1 and HI-2. Examination of Tables 13 and 14 shows that it was the least abundant fission product on the cladding (expressed as a fraction of inventory), and generally less was present on the end caps; this confirms that ^{144}Ce remained with the fuel. Europium-154 was also detected by gamma counting and appeared to follow ^{144}Ce closely in behavior since it is chemically similar. However, we did not use it as a fuel marker because of its tendency to form a stable Eu^{2+} ion and to volatilize as europium metal when fuel is heated with metallic Zircaloy, as is the case with strontium and barium.¹²

To remove the effects of fission product movement with fuel dust, it is necessary to define an enrichment. For example,

Table 13. Activities^a of cladding and end-cap samples from test HI-1

Isotope	Original sample		Cladding after H ₂ O rinse		End cap after H ₂ O rinse		Activity loss (% of original sample)	
	(μ Ci)	(% of inventory)	(μ Ci)	(% of inventory)	(μ Ci)	(% of inventory)	In handling and rinsing	On end cap
⁵⁴ Mn	326		71.2				78	0
⁶⁰ Co	86.3		42.1		19.4		29	22
¹⁰⁶ Ru	4850	0.04	1080	0.0098	2980	0.027	16	61
^{110m} Ag ^b	1480	4	482	1.35	<123	<0.34	59	<8
¹²⁵ Sb	1260	(0.15) ^c	966	(0.112) ^c	464	0.054	0	37
¹³⁴ Cs	1960	0.031	288	0.0045	1210	0.019	24	62
¹³⁷ Cs	3260	0.032	453	0.0045	2000	0.020	25	61
¹⁴⁴ Ce	2500	0.019	421	0.0032	1280	0.0099	32	51
¹⁵⁴ Eu	134	0.016	15.5	0.0018	92.1	0.011	20	69
¹⁵⁵ Eu	38.2		3.28		21.2		36	56

^aActivities in microcuries, as of Nov. 2, 1976.

^bSubject to very large errors because of counting statistics; silver activity, when counted, was less than 10% of the next strongest activity.

^cPercentages include contributions from activation of tin in Zircaloy cladding.

Table 14. Activities^a of cladding and end-cap samples from test HI-2

Isotope	Original sample		Cladding after H ₂ O rinse		End cap after H ₂ O rinse		Activity loss (% of original sample)	
	(μ Ci)	(% of inventory)	(μ Ci)	(% of inventory)	(μ Ci)	(% of inventory)	In handling and rinsing	On end cap
⁶⁰ Co	15.2		6.82		6.70		11	44
¹⁰⁶ Ru	765	0.2	687	0.16	31.8	0.0074	6	4
^{110m} Ag ^b	~2	~0.7	<3	<1	~2	~0.7		
¹²⁵ Sb	1110	(0.4) ^c	167	(0.064) ^c	968	0.37	0	87
¹³⁴ Cs	626	0.05	317	0.025	272	0.022	6	43
¹³⁷ Cs	3990	0.04	2110	0.024	1780	0.020	3	45
¹⁴⁴ Ce	53.0	0.03	46.7	0.024	5.69	0.0029	1	11
¹⁵⁴ Eu	619	0.11	611	0.104	22.9	0.0039	0	4

^aActivities in microcuries, as of July 15, 1981.

^bSubject to very large errors because of counting statistics.

^cPercentages include contributions from activation of tin in Zircaloy cladding.

enrichment of $^{137}\text{Cs} = \frac{\text{fraction of fuel inventory of } ^{137}\text{Cs on component}}{\text{fraction of fuel inventory of } ^{144}\text{Ce on component}} .$

Tables 15 and 16 give the enrichments for tests HI-1 and HI-2. Since all the fission products were enriched relative to ^{144}Ce in both HI-1 and HI-2, they probably migrated independently of fuel particles. The alternative is that they were enriched by recoil; however, this would imply that ^{144}Ce precursor nuclei are ejected more slowly than any other nuclei, which is improbable. This hypothesis would also lead to enrichment of the cladding, but not of the end caps since these were added long after the active life of the fuel.

Ruthenium-106 was enriched twofold to threefold in both HI-1 and HI-2; only the cladding in HI-2 was more highly enriched (by a factor of 7). Ruthenium may be slightly volatile as an oxide in steam atmospheres,¹³ but this volatility is less in reducing atmospheres such as those in HI-1 and HI-2. At present, the most plausible explanation of the ^{106}Ru measurements is a combination of vapor transport as a volatile species and diffusion through the fuel, across the interface and into the cladding in HI-2.

The silver values are in disagreement. Silver has a great affinity for Zircaloy,¹⁴ which is reflected in the enrichments measured in tests HI-1 and HI-2. Silver metal vaporized from the fuel and was absorbed into the Zircaloy cladding. The end cap in test HI-1 was further from the fuel and hence collected less silver vapor. In test HI-2, however, more silver remained on the end cap than on the cladding. The cladding was more than 80% oxidized to ZrO_2 , and apparently the silver was driven off during oxidation, while the thicker end cap resisted oxidation and retained silver.

Antimony-125 is present as a decay product in irradiated Zircaloy, and this accounts for the enrichment in HI-1 cladding. The enrichments in tests HI-1 and HI-2 end caps reflect the volatility of antimony at 1400 to 1700°C; antimony vapor has left the fuel and been absorbed into the end caps. Apparently, extensive oxidation of the Zircaloy cladding in test HI-2 reduced the enrichment (cf. silver, above).

The enrichment values show that cesium vaporized from the fuel and condensed on the cladding and end caps. Little interaction occurred between the Zircaloy and its oxides at 1400 and 1700°C; most of the cesium left the fuel area completely and condensed elsewhere in the apparatus. There was no clear reason for the difference in enrichments for the cladding and the end cap in HI-2. Cesium appeared to favor ZrO_2 environments and thus is expected to stay with the cladding, not the end cap.

Europium-154 was enriched in the HI-2 cladding (which was in contact with fuel), but not in the end cap. Gaseous diffusion of species such as europium atoms is not responsible because enrichment on the end cap would be observed in this case. The most plausible explanation is solid-state

Table 15. Enrichment of nuclide relative to fuel dust
(^{144}Ce and ^{154}Eu) in HI-1

Nuclide	Enrichment ratio of nuclide	
	In cladding	In end cap
^{106}Ru	2-3	2-3
$^{110\text{m}}\text{Ag}$	400	40
^{125}Sb	35	5
$^{134}, ^{137}\text{Cs}$	2	2

Table 16. Enrichment of nuclide relative to fuel dust
(^{144}Ce) in HI-2

Nuclide	Enrichment ratio of nuclide	
	In cladding	In end cap
^{106}Ru	7	2
$^{110\text{m}}\text{Ag}$	40	250
^{125}Sb	3	100
$^{134}, ^{137}\text{Cs}$	1	7
^{154}Eu	4	1

diffusion of europium through the uranium oxide-Zircaloy matrix. Europium forms stable Eu^{2+} ions, which are large and may strain the UO_2 lattice sufficiently to enhance diffusion. Since cerium has no stable oxidation state lower than Ce^{3+} , it will diffuse slowly.

The loss of a large proportion of the ^{54}Mn detected in the cladding sample from test HI-1 during handling and rinsing prevents us from drawing definitive conclusions concerning the behavior of manganese. No manganese was found in the HI-2 cladding samples; it may have completely evaporated during the heating cycle since it is quite volatile (vapor pressure = 0.066 bar at 1700°C).

Cobalt-60 transferred from the cladding to the end caps in both HI-1 and HI-2, indicating slight volatility (vapor pressure = 2.6×10^{-5} bar at 1700°C).

3.2.5.2 Metallographic examination of fuel specimens

After being cast in epoxy resin to preserve their physical shapes, the fuel specimens from tests HI-1 and HI-2 were transferred to another hot cell facility and sectioned for detailed examination of the microstructures. One radial section from test HI-1 and two radial sections from test HI-2 were selected and prepared by standard metallographic techniques.

The specimen from test HI-1 (1400°C for 30 min) is shown in Fig. 16. Several cladding fractures are apparent in this specimen, which was located at 8.3 cm from the inlet end of the fuel rod. The microstructure in the region of a fracture is compared with an untested control specimen in Fig. 17. Successive layers of ZrO_2 , oxygen-stabilized α -zirconium, and a thin layer of ZrO_2 on the inner surface of the cladding are identified. The thin layer of ZrO_2 on the fracture surfaces (relative to the outer surface) indicates that the fractures occurred late in the heating cycle, perhaps at the beginning of cooldown. Similarly, the relatively thin layer of ZrO_2 on the inside surface of the cladding shows that the atmosphere in this region of the fuel specimen was reducing throughout most of the high-temperature period. The same area is shown in polarized light in Fig. 18, which shows the large grain size in the α -ZrO region. The thickness of the ZrO_2 layer on the outside of the cladding agreed well with the work of Pawel¹⁵ and indicated that about 40% of the zirconium at this location had been converted to ZrO_2 . The test caused no visible change in the UO_2 fuel. These results are also consistent with the observations of Cook¹⁶ and Kerwin¹⁷ of in-pile fuel tests under similar conditions.

Two metallographic specimens were selected, at 5.8 and 17.7 cm from the inlet end of the HI-2 fuel rod; the latter is displayed in Fig. 19. The sketch in Fig. 20 indicates the relative locations of the large cladding fracture in the specimen and the cross sections examined. The cladding adjacent to the fractures is shown in Fig. 21; the essentially complete oxidation to ZrO_2 apparent in this view was typical of both specimens from this test and illustrates the more severe damage as a

ORNL PHOTO 4183-83

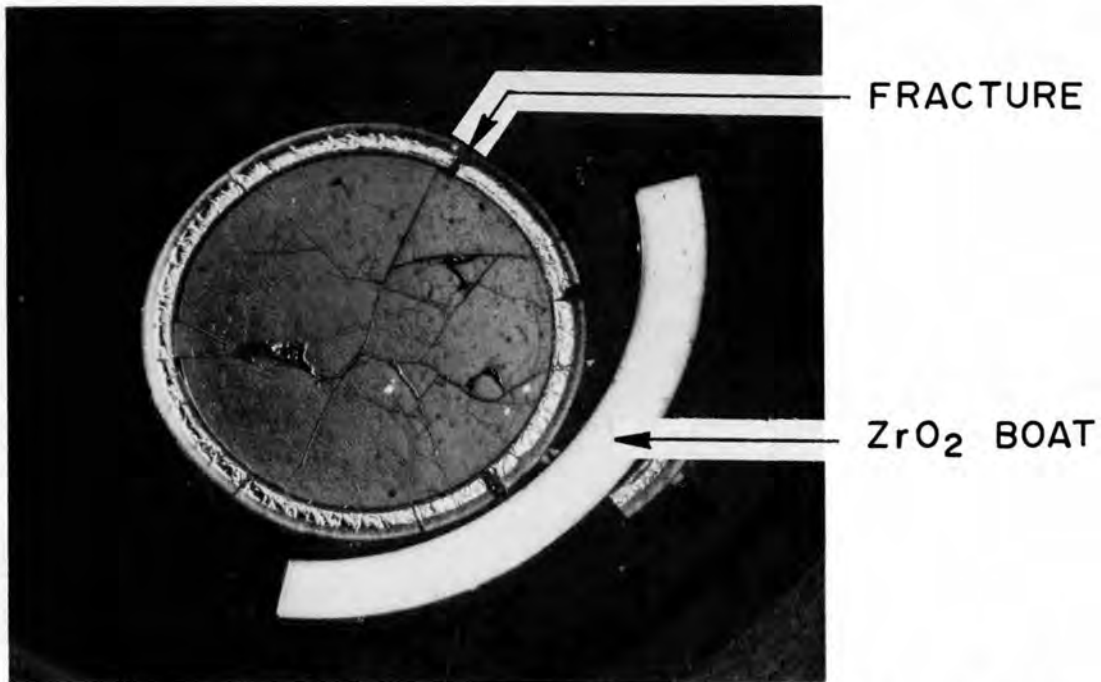


Fig. 16. Appearance of metallographic specimen from test HI-1, showing cladding fractures and ZrO_2 boat ($\sim 4.8\times$).

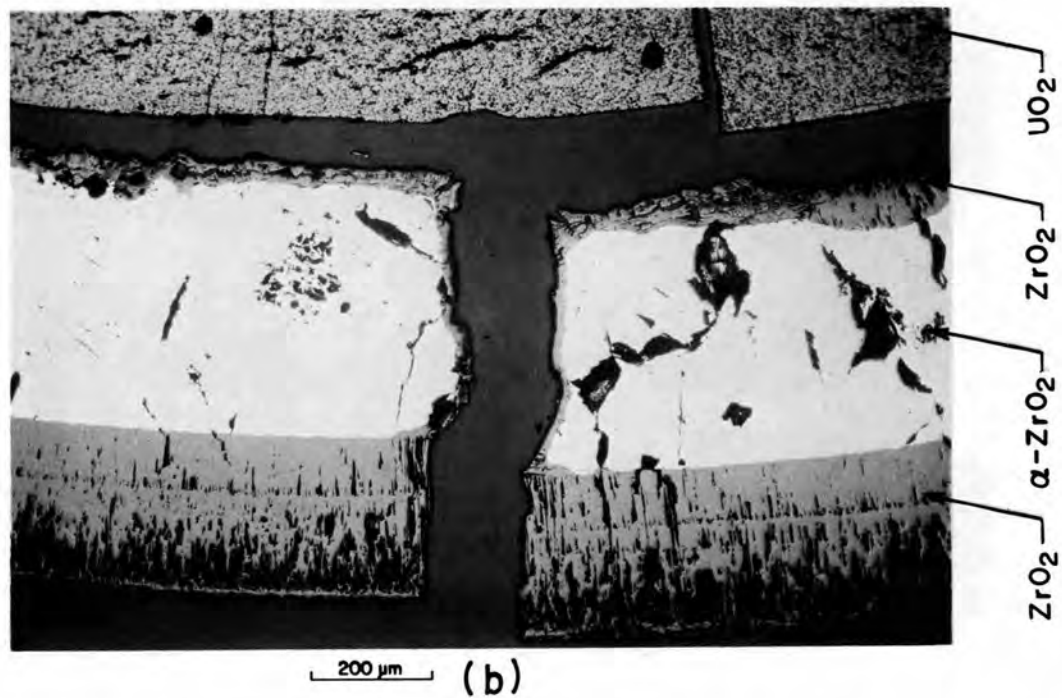
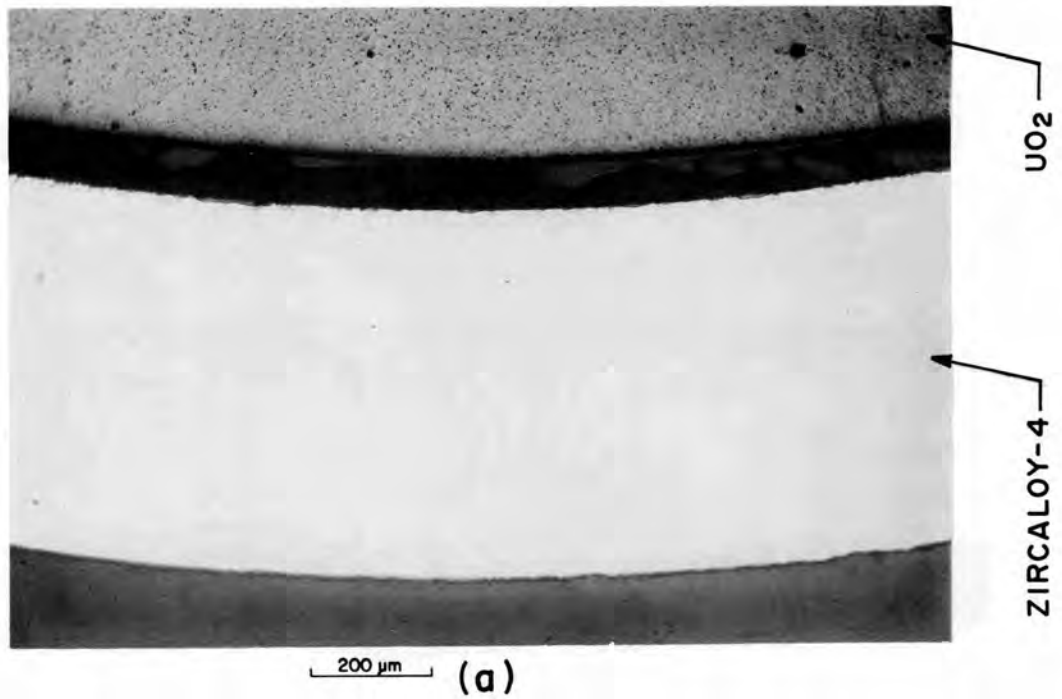


Fig. 17. Comparison of (a) cladding appearance in irradiated but untested control specimen with (b) that in test HI-1. Note fracture, the increase in thickness, and the ZrO₂ and α-ZrO layers resulting from the conditions used for the test.

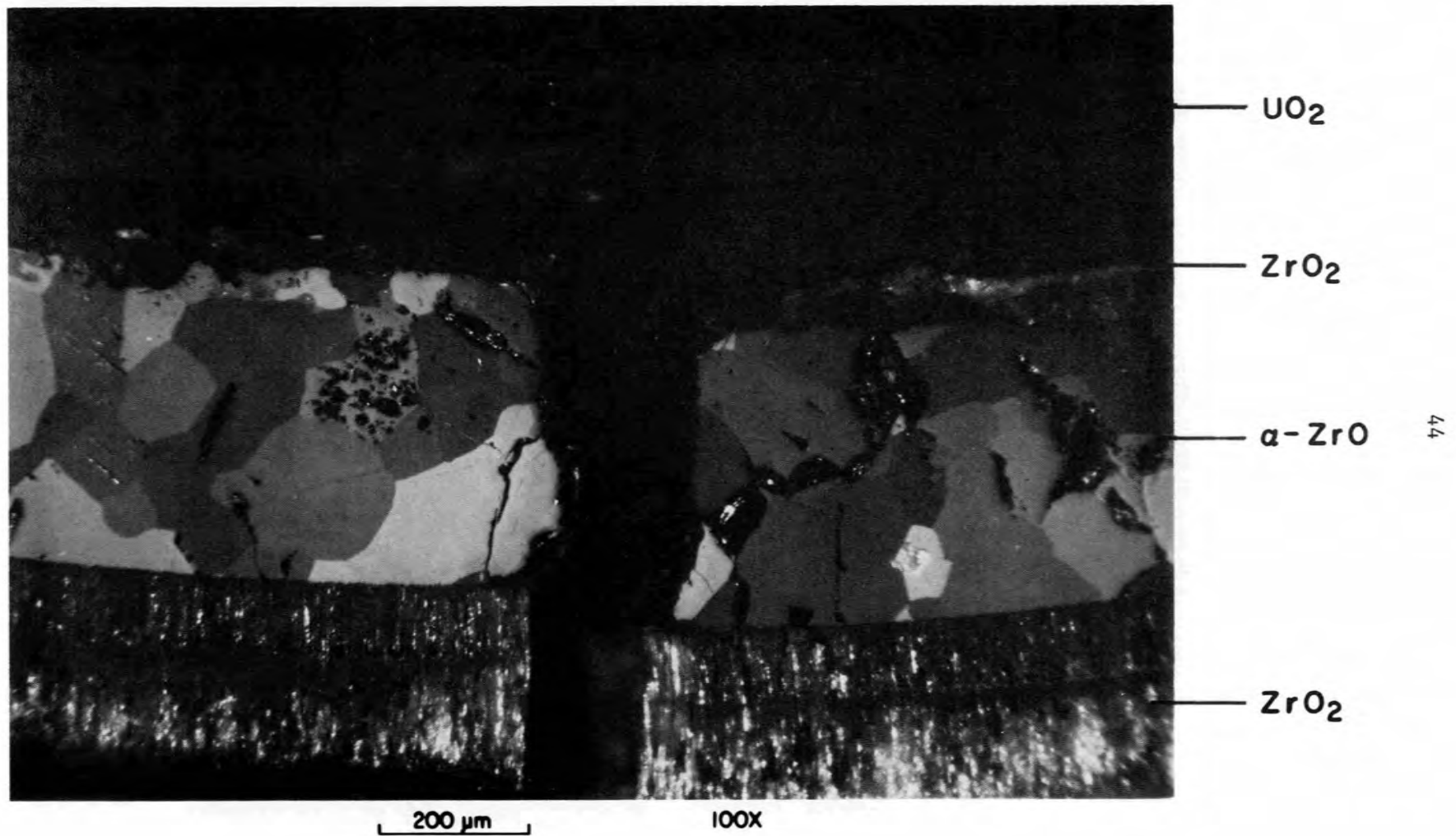
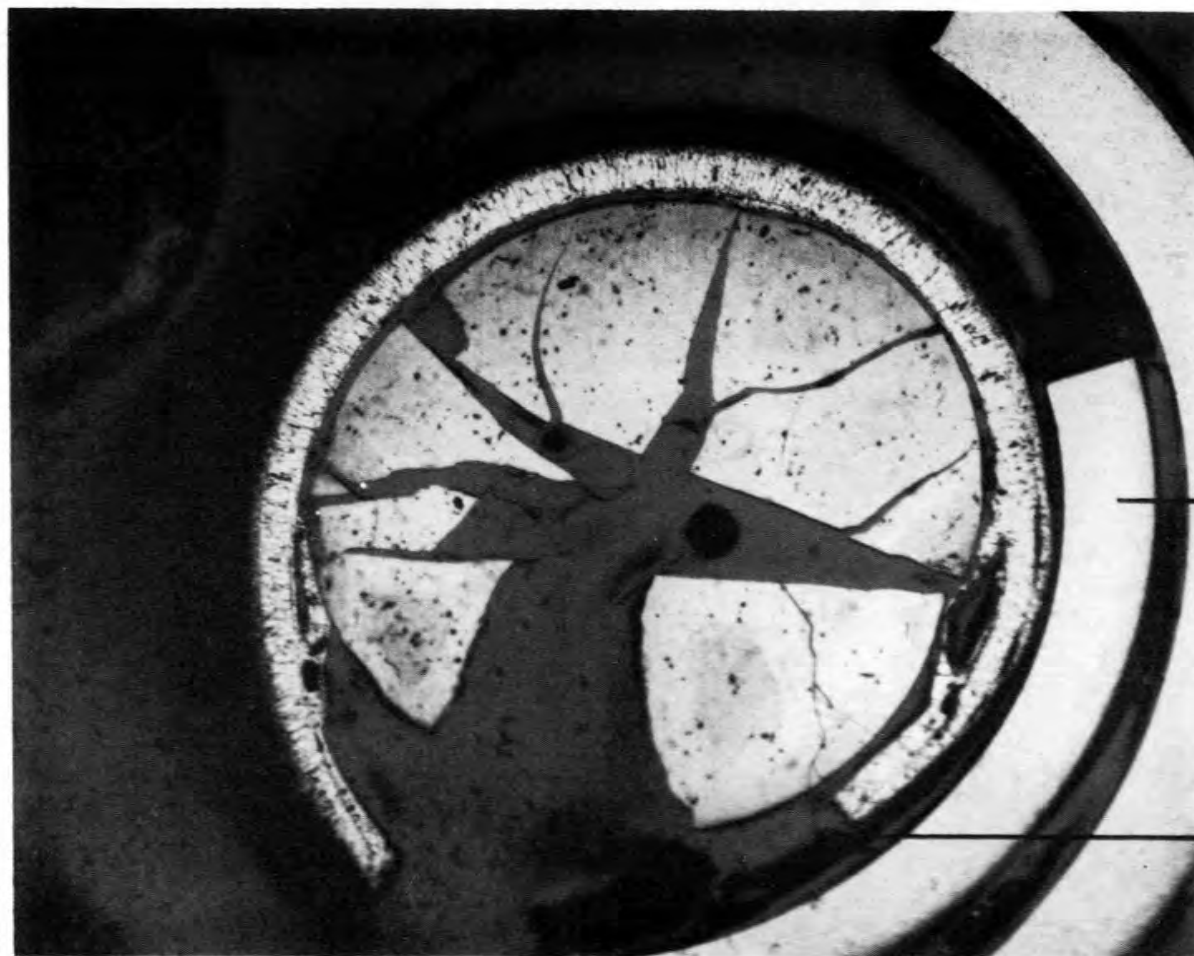


Fig. 18. Appearance of test HI-1 specimen under polarized light, which makes grain structures visible.

ORNL PHOTO 3438-83



ZrO₂ BOAT

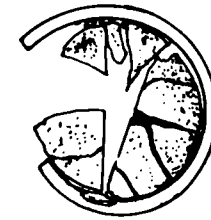
FRACTURE

45

Fig. 19. Appearance of metallographic specimen from test HI-2, showing wide opening at cladding fracture (~5 \times).



SECTION A



SECTION B

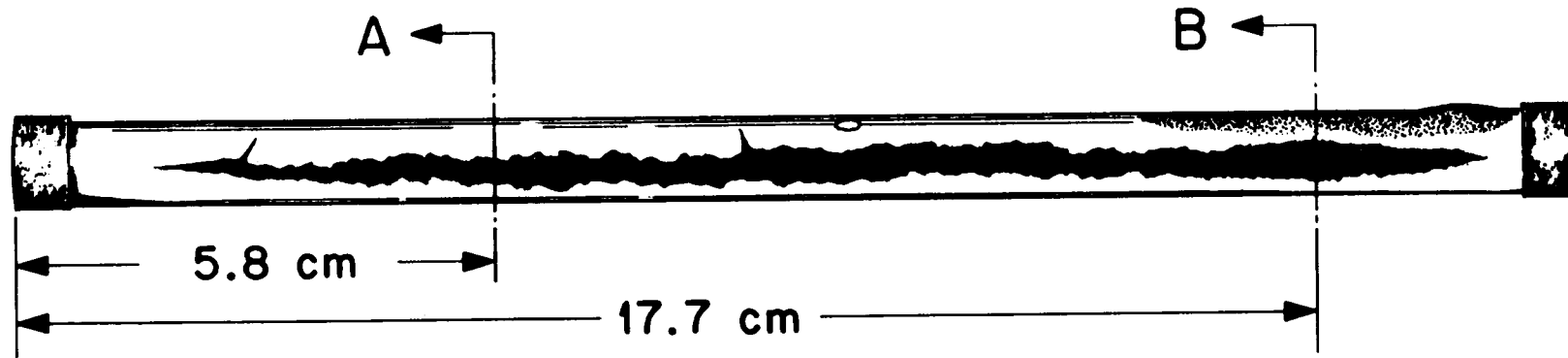


Fig. 20. Sketch of HI-2 fuel specimen after test, showing large longitudinal fracture, unidentified dark spot on downstream end of specimen, and locations of cuts for metallographic examination.

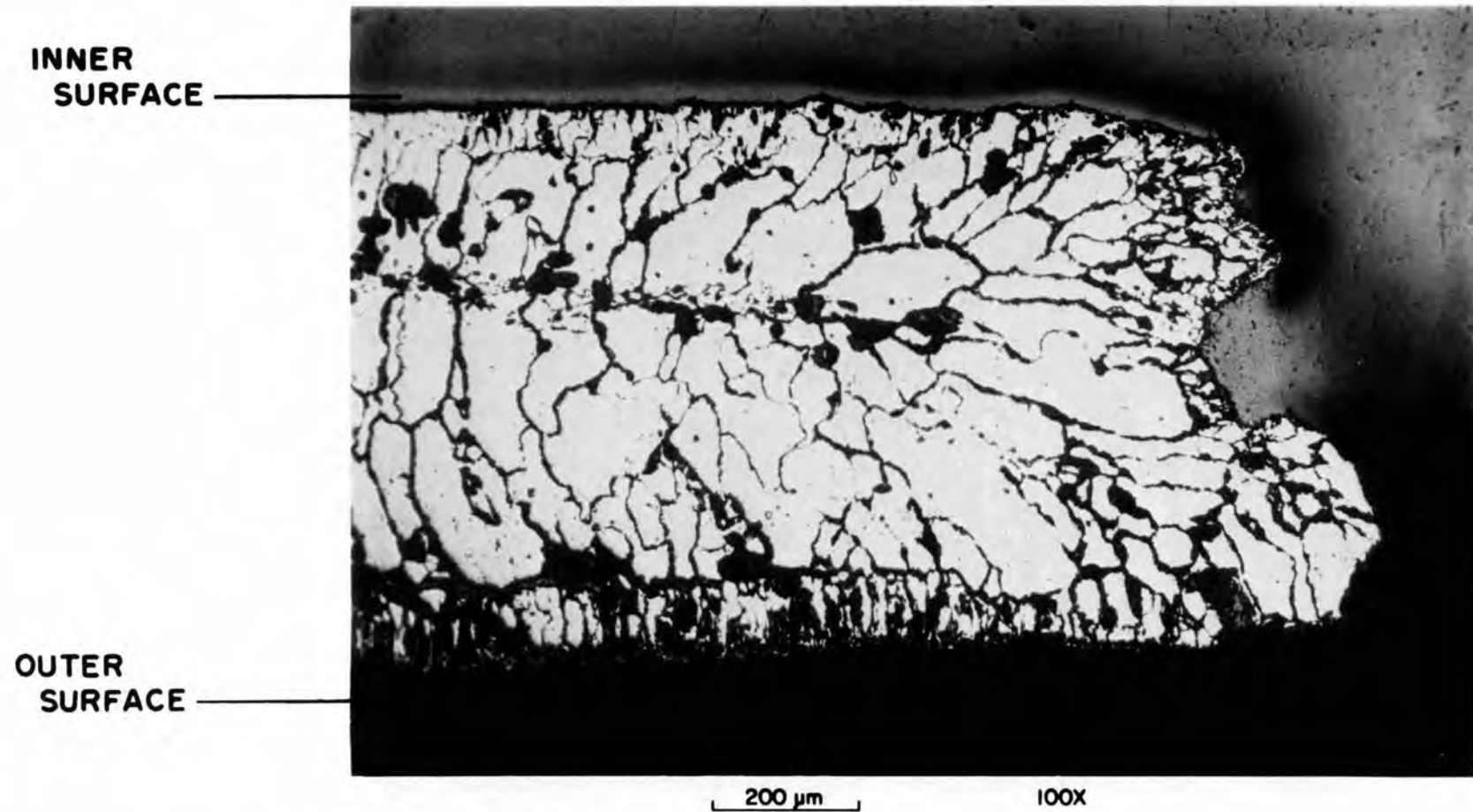


Fig. 21. Completely oxidized cladding adjacent to fracture in test HI-2.

result of the higher test temperature (1700 vs 1400°C). Further effects are shown in Figs. 22 and 23. Fine precipitates of metallic tin, which are to be expected under the conditions used in test HI-2, are apparent in Fig. 22; and a chip of UO₂ adhering to the cladding, indicative of fuel-cladding interaction, is shown in Fig. 23. Neither of these phenomena was observed in the lower-temperature test, but Hofmann et al.¹⁸ have studied UO₂-zirconium interactions at 1600°C.

These metallographic specimens and additional sections from the fuel rods were shipped to Argonne National Laboratory for further, more detailed investigations of the microstructures and chemical compositions.

4. CONCLUSIONS

As indicated in Sect. 1, this summary report presents only a limited evaluation and interpretation of the data obtained in test HI-2. Further evaluation, interpretation, and correlation will be included in a topical report, which will consider the results of several tests over a range of experimental conditions. Therefore, our current conclusions are of a preliminary nature and must be restricted to the following observations:

1. The experimental apparatus performed satisfactorily, and the techniques and equipment appear to be suitable for further testing up to 2000°C.
2. The on-line release rate measurements for ⁸⁵Kr and ¹³⁷Cs (Fig. 9) appear to be consistent both with the prior test in this series and with previous work. The increase in release rates for both krypton and cesium at the beginning of specimen cooldown agreed with such observations by other experimenters.¹⁹
3. The appearance of the fuel specimen after the test was similar to that of unirradiated specimens under the same conditions. The Zircaloy cladding was almost completely oxidized to ZrO₂, in agreement with hydrogen generation data from flow measurements, and a large fracture extended over about 80% of the length of the specimen.
4. Based on gamma-ray spectrometry of fission product nuclides, 52.5% of the krypton, 50.5% of the cesium, 1.55% of the antimony, and 2.59% of the silver were released from the specimen during the test. Activation analysis indicated that 53.8% of the iodine was released, which is in good agreement with the values for krypton and cesium. All of these results appear to be reasonably consistent both with earlier work by Lorenz et al.²⁻⁴ and with a recent NRC-sponsored review of relevant data.¹³
5. Data obtained from SSMS analyses of smear and solution samples from selected locations corroborated the gamma analysis results and also provided some additional information concerning stable fission product elements, such as Te, Mo, and Rb, as well as structural and impurity elements, most notably W (susceptor) and Sn (cladding).

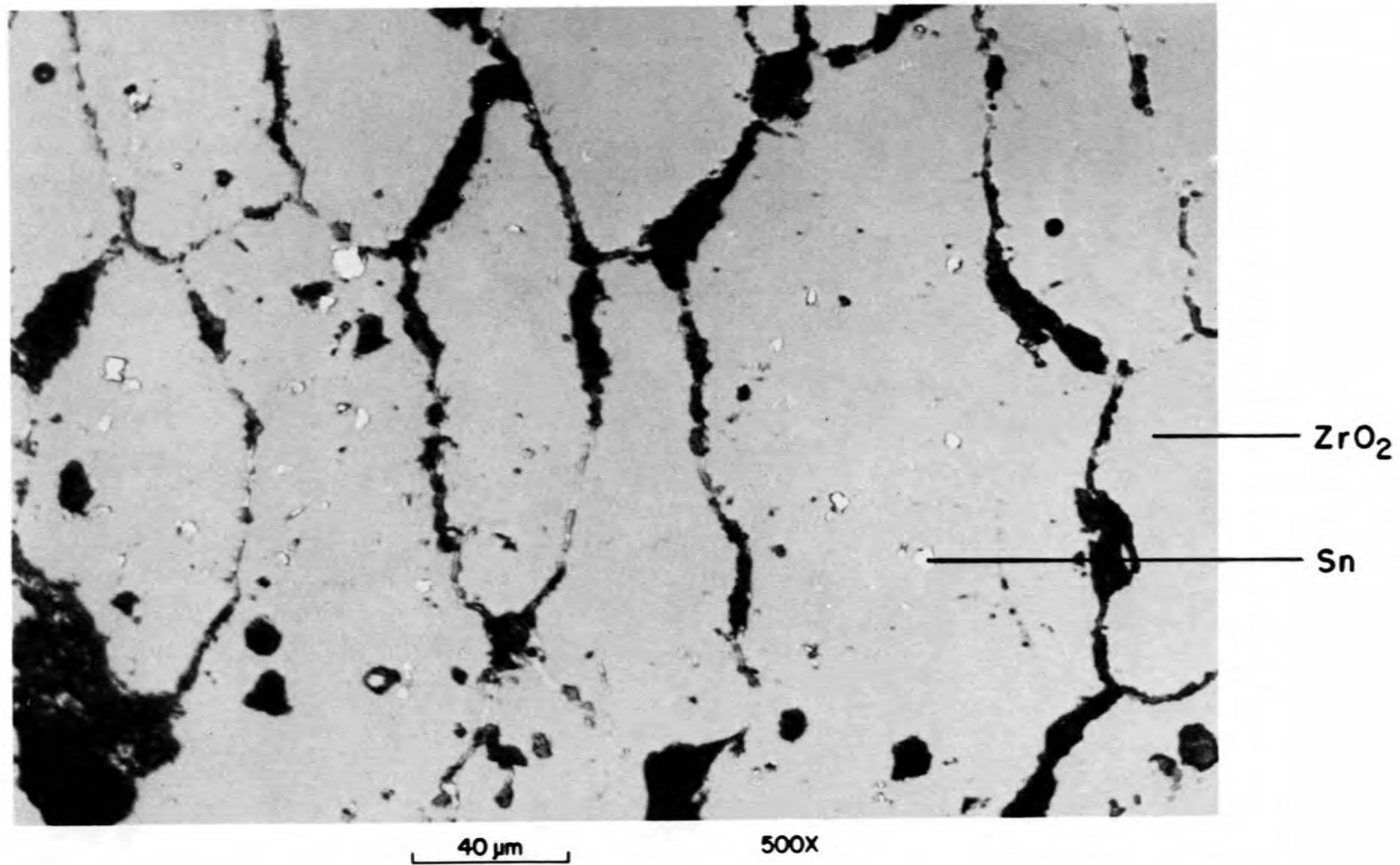


Fig. 22. Higher-magnification view from central region of test HI-2 cladding, showing precipitates of metallic tin.

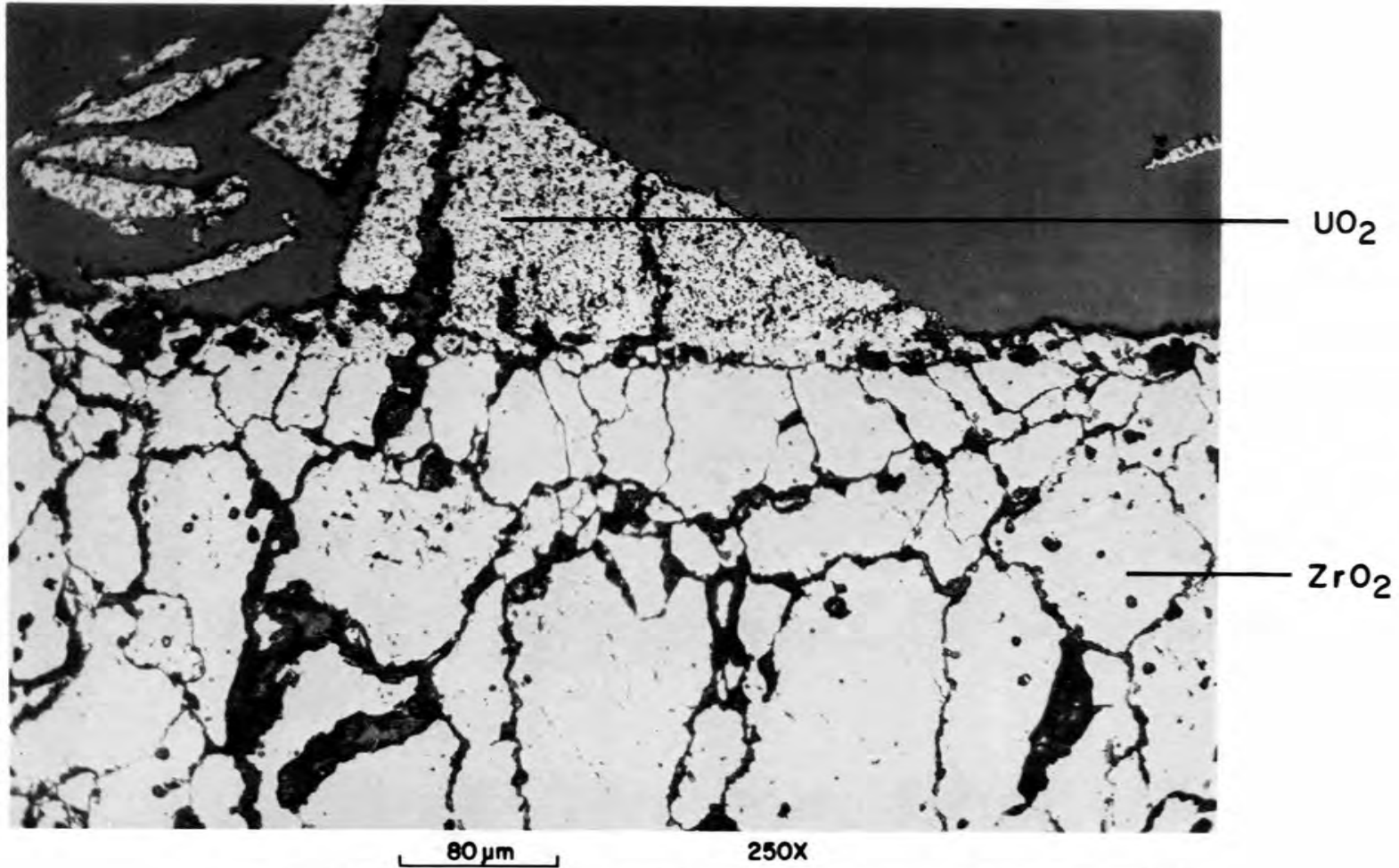


Fig. 23. Area of apparent fuel-cladding interaction in test HI-2, showing chip of UO_2 fuel adhering to oxidized Zircaloy cladding.

6. Evaluation of data for Cs, I, Sb, and Ag on the thermal gradient tube provided some information about the chemical forms of these fission products. Cesium exhibited a complex behavior, probably indicating its presence as two or more compounds; CsOH is the most likely form in our system. Iodine appeared to be associated with cesium, perhaps as CsI. Antimony behaved like the element, alloying with the platinum thermal gradient tube, while silver exhibited characteristics typical of both a compound (at 400-900°C) and the element (below 400°C).
7. Metallographic examination of sections from tests HI-1 and HI-2 revealed that oxidation and embrittlement of the Zircaloy cladding were more severe in the higher-temperature test (HI-2 operated at 1700°C vs 1400°C for HI-1); in addition, evidence of limited fuel-cladding interaction was observed. Such phenomena are not unexpected at this temperature. The microstructures will be examined in greater detail at a later date and will be reported in conjunction with subsequent tests.

5. REFERENCES

1. M. F. Osborne, R. A. Lorenz, and R. P. Wichner, "Program Plan for Fission Product Release from LWR Fuel in Steam," memorandum to USNRC, April 1982.
2. R. A. Lorenz, J. L. Collins, A. P. Malinauskas, O. L. Kirkland, and R. L. Towns, Fission Product Release from Highly Irradiated LWR Fuel, NUREG/CR-0722 (ORNL/NUREG/TM-287/R2) (February 1980).
3. R. A. Lorenz, J. L. Collins, A. P. Malinauskas, M. F. Osborne, and R. L. Towns, Fission Product Release from Highly Irradiated LWR Fuel Heated to 1300-1600°C in Steam, NUREG/CR-1386 (ORNL/NUREG/TM-346) (November 1980).
4. R. A. Lorenz, J. L. Collins, M. F. Osborne, R. L. Towns, and A. P. Malinauskas, Fission Product Release from BWR Fuel Under LOCA Conditions, NUREG/CR-1773 (ORNL/NUREG/TM-388) (July 1981).
5. R. A. Lorenz, J. L. Collins, and A. P. Malinauskas, Fission Product Source Terms for the LWR Loss-of-Coolant Accident, NUREG/CR-1298 (ORNL/NUREG/TM-321) (July 1980).
6. M. F. Osborne, R. A. Lorenz, J. R. Travis, and C. S. Webster, Data Summary Report for Fission Product Release Test HI-1, NUREG/CR-2928 (ORNL/TM-8500) (December 1982).
7. P. E. MacDonald to A. P. Malinauskas, Transmittal of CPL Assembly B05 Axial Flux Measurements, MacD-76-75 (Sept. 11, 1975).
8. M. F. Osborne and G. W. Parker, The Effect of Irradiation on the Failure of Zircaloy-Clad Fuel Rods, ORNL-TM-3626 (January 1972).

9. H. Albrecht, M. F. Osborne, and H. Wild, "Experimental Determination of Fission and Activation Product Release During Core Meltdown," Proceedings of Thermal Reactor Safety Meeting, Sun Valley, Idaho, Aug. 1-4, 1977.
10. T. B. Lindemer, ORNL, personal communication to K. S. Norwood, 1982.
11. M. Hansen, Constitution of Binary Alloys, pp. 1138-39, McGraw-Hill, New York, 1958.
12. G. W. Parker et al., Out-of-Pile Studies of Fission-Product Release from Overheated Reactor Fuels at ORNL, 1955-1965, ORNL-3981 (July 1967).
13. Technical Bases for Estimating Fission Product Behavior During LWR Accidents, NUREG-0772, U.S. Nuclear Regulatory Commission (June 1981).
14. S. Hagen et al., Projekt Nukleare Sicherheit Halbjahresbericht, KfK-2750 (November 1978).
15. R. E. Pawel, ORNL, personal communication, February 1983.
16. B. A. Cook, Fuel Rod Material Behavior During Test PCM-1, NUREG/CR-0757 (June 1979).
17. D. K. Kerwin, Test PCM-5 Fuel Rod Materials Behavior, NUREG/CR-1430 (May 1980).
18. P. Hofmann, D. Kerwin-Peck, and P. Nikolopoulos, "Physical and Chemical Phenomena Associated with the Dissolution of Solid UO_2 by Molten Zircaloy-4," paper presented at the Sixth International Conference on Zirconium in the Nuclear Industry, June 28-July 1, 1982, Vancouver, British Columbia, Canada.
19. R. M. Carroll and O. Sisman, Evaluating Fuel Behavior During Irradiation by Fission Gas Release, ORNL-4601 (September 1970).

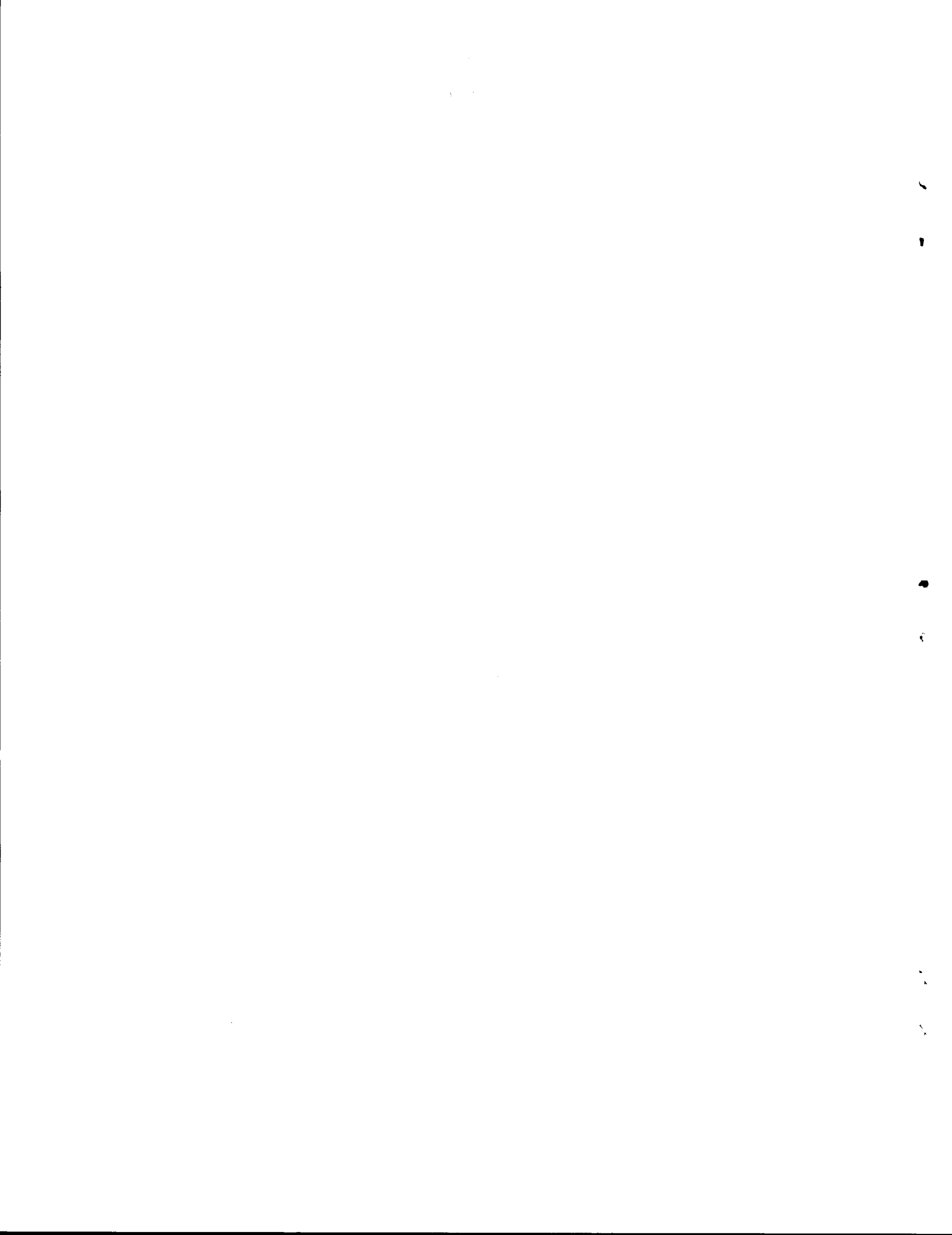
NUREG/CR-3171
ORNL/TM-8667
Dist. Category R3

INTERNAL DISTRIBUTION

- | | | | |
|--------|-------------------|--------|---|
| 1. | R. E. Adams | 27. | J. H. Shaffer |
| 2. | C. W. Alexander | 28. | R. D. Spence |
| 3. | E. C. Beahm | 29. | M. G. Stewart |
| 4. | J. T. Bell | 30. | O. K. Tallent |
| 5. | R. H. Chapman | 31. | R. L. Towns |
| 6. | J. L. Collins | 32-33. | J. R. Travis |
| 7. | G. E. Creek | 34-36. | C. S. Webster |
| 8. | T. S. Kress | 37. | S. K. Whatley |
| 9. | C. E. Lamb | 38. | R. P. Wichner |
| 10. | T. B. Lindemer | 39. | A. L. Wright |
| 11-13. | R. A. Lorenz | 40. | R. G. Wymer |
| 14. | A. L. Lotts | 41. | Central Research Library |
| 15. | A. P. Malinauskas | 42. | ORNL-Y-12 Technical Library
Document Reference Section |
| 16. | J. W. Nehls | 43. | Laboratory Records |
| 17-19. | K. S. Norwood | 44. | Laboratory Records, ORNL RC |
| 20-24. | M. F. Osborne | 45. | ORNL Patent Section |
| 25. | G. W. Parker | | |
| 26. | D. J. Pruett | | |

EXTERNAL DISTRIBUTION

46. Office of Assistant Manager, Energy Research and Development,
DOE-ORO, P.O. Box E, Oak Ridge, TN 37831
- 47-48. Director, Division of Reactor Safety Research, Nuclear
Regulatory Commission, Washington, DC 20555
- 49-50. Technical Information Center, Oak Ridge, TN 37830
- 51-325. Given distribution as shown in Category R3 (NTIS - 10)



NRC FORM 335 <small>(11-81)</small>		U.S. NUCLEAR REGULATORY COMMISSION BIBLIOGRAPHIC DATA SHEET		1. REPORT NUMBER (Assigned by DDC) NUREG/CR-3171 (ORNL/TM-8667)	
4. TITLE AND SUBTITLE (Add Volume No., if appropriate) Data Summary Report for Fission Product Release Test HI-2				2. (Leave blank)	
7. AUTHOR(S) M. F. Osborne, R. A. Lorenz, J. R. Travis, C. S. Webster, and K. S. Norwood				3. RECIPIENT'S ACCESSION NO.	
9. PERFORMING ORGANIZATION NAME AND MAILING ADDRESS (Include Zip Code) Oak Ridge National Laboratory P.O. Box X Oak Ridge, TN 37830				5. DATE REPORT COMPLETED MONTH YEAR January 1983	
12. SPONSORING ORGANIZATION NAME AND MAILING ADDRESS (Include Zip Code) Division of Accident Evaluation Office of Nuclear Regulatory Research U. S. Nuclear Regulatory Commission Washington, D. C. 20555				6. (Leave blank)	
13. TYPE OF REPORT Data Summary				PERIOD COVERED (Inclusive dates) June 1982 — January 1983	
15. SUPPLEMENTARY NOTES				8. (Leave blank)	
16. ABSTRACT (200 words or less) <p>The second in a series of high-temperature fission product release tests was conducted for 20 min at about 1700°C in flowing steam. The test specimen, a 20-cm-long section of an H. B. Robinson fuel rod that had been irradiated to a burnup of 28,000 MWd/t, was heated in an induction furnace mounted in a hot cell.</p> <p>Posttest analyses of the furnace, the thermal gradient tube, filters, and other components of the experimental apparatus showed that about 50% of the ^{85}Kr, ^{137}Cs, and ^{129}I were released from the specimen during the test. In addition, approximately 2% of the ^{110m}Ag and ^{125}Sb along with smaller fractions of several other radionuclides were measured by gamma spectrometry. Spark-source mass spectrometric data from a limited number of samples showed significant releases of fission product tellurium and molybdenum, as well as structural (zirconium and tin) and furnace (primarily tungsten) materials. Metallographic examination of the fuel specimen revealed extensive fractures in the cladding, essentially complete oxidation to ZrO_2, and evidence of fuel-cladding interaction.</p>				10. PROJECT/TASK/WORK UNIT NO.	
17. KEY WORDS AND DOCUMENT ANALYSIS Fission product Fission product release				11. FIN NO. B0127	
17b. IDENTIFIERS: OPEN-ENDED TERMS				14. (Leave blank)	
18. AVAILABILITY STATEMENT		19. SECURITY CLASS (This report) Unclassified		21. NO. OF PAGES	
		20. SECURITY CLASS (This page) Unclassified		22. PRICE S	